External Transmittal
Authorized

Distribution Limited To
Recipients Indicated

ORNL-CF-60-7-76

CHEMICAL TECHNOLOGY DIVISION

MONTHLY PROGRESS REPORT FOR CHEMICAL DEVELOPMENT SECTION B

JUNE - JULY 1960

R. E. Blanco

DATE ISSUED

DEC 12 1960

OAK RIDGE NATIONAL LABORATORY
Operated by
UNION CARBIDE NUCLEAR COMPANY
for the
U.S. ATOMIC ENERGY COMMISSION

DISCLAIMER

ABSTRACT

Dissolution of Consolidated Edison Fuel

The effect of two neutron poisons, boron and cadmium, on the rate of dissolution of high density 95% ThO_2-UO_2 pellets in boiling 13 M HNO_3--0.04 M NaF--0 to 0.1 M $Al(NO_3)_3$ was determined. Initial 10-min rates were independent of boric acid concentration up to 0.1 M, but an attempt to prepare by dissolution a solution containing 1 M thorium, and 0.1 M boric acid resulted in the precipitation of $Th(NO_3)_4$. Surprising results were obtained with solutions containing cadmium in that the initial 10-min rate in dissolvent containing no aluminum decreased from 2 to 0.7 mg $min^{-1}cm^{-2}$, but, in dissolvent containing 0.1 M aluminum, the rate increased from 0.7 to 2 mg $min^{-1}cm^{-2}$ with the same change in cadmium concentration.

Dissolution of Uranium-Molybdenum Alloy Fuels

Dissolution of U-10% Mo alloy in boiling nitric acid to produce 1 M uranium solutions resulted in precipitation of uranyl molybdates, e.g. $UO_3 \cdot 2\ MoO_3$, at low acidities, but MoO_3 at final acidities greater than 5 M.

Effect of Air and Irradiation on Uranium and Thorium Losses During Decladding of Consolidated Edison Fuel

Exposure of refluxing final Sulfex and Darex decladding solutions to air while contacting nonirradiated Consolidated Edison pellets caused the uranium losses to double and more than triple, respectively, at 3 hr contact time and to increase at about 0.01 and 0.05%/hr, respectively, after 3 hr. In contrast, losses caused by Co^{60} radiation in similar solutions in the absence of air at a radiant power density of about 1 watt/liter were not large enough to measure accurately.

Processing of U-Mo Fuel by A Zircex-type Process

An alloy of 91.6% U-Mo reacted with 10-90% HCl-air at 400-600°C at rates of 8-10 mg/cm^2-min and with chlorine at furnace temperatures above 450°C at a rate of 20 mg/cm^2-min. Volatilization of 98% and 90% of the molybdenum was achieved with chlorine and mixed hydrogen chloride-air, respectively. Adding air to hydrogen chloride doubled the reaction rate and caused volatilization of over 99% of the chloride from the product. Aluminum reacted with both hydrogen chloride and chlorine at a furnace temperature of 300°C at a rate of 11 mg/cm^2-min. Stainless steel reacted with chlorine at 600°C at a rate of 0.55 mg/cm^2-min.

Recovery of Uranium from Graphite Fuels

Graphitized and ungraphitized 1.5-in. dia spheres of admixture type prototype Pebble Bed reactor fuels were disintegrated to -10 mesh powder by treating with 90% HNO_3 at either 25°C or the reflux temperature. The graphitized specimens disintegrated more rapidly than the ungraphitized.

The outer layers of both fuel types disintegrated more rapidly than the central core (84% of the graphitized fuel in 7 hr, but 24 hr for complete disintegration; 65% of the ungraphitized fuel in 7 hr, but only about 95% after 24 hr). Powder was removed from the mixture after 6-10 hr to avoid the formation of very fine particles which were difficult to filter. After partially disintegrated material had been washed with water, no further disintegration occurred upon subsequent treatment with 90% acid. Two leaches with 90% HNO_3 —one of which is the disintegration step — and thorough washing of the graphite with either water or HNO_3 recovered 99% or more of the uranium in the powder. When complete disintegration did not occur, only 30% of the uranium was leached from the core. Grinding these fuels to -4+8 mesh and leaching with boiling 70% acid recovered only 97.6% of the uranium. Grinding a Si-SiC coated, ungraphitized prototype to -200 mesh and leaching with 70% HNO_3, or grinding to -4+8 mesh and leaching with 90% acid recovered 99% of the uranium.

Solvent Extraction Studies

Irradiation of synthetic Consolidated Edison fuel solution to 5 and 10 watt-hr per liter in a Co^{60} source resulted in about a 50% decrease in decontamination factor using the Acid-Thorex flowsheet. After irradiation to 60-165 watt-hr per liter the decontamination factor improved by factors of 2 and 5, respectively. Decreasing the TBP concentration from 15 to 5% in the final uranium purification cycle, at a uranium saturation of 61 to 68% increased the fission product decontamination factor by a factor of 2. The decontamination factor decreased by a factor of 5, however, on further decrease of TBP concentration to 2.5% at a uranium saturation of 38%. This indicates a stronger dependence on saturation than on TBP concentration.

Corrosion Studies

After 48 Thorex FAT batch boildowns negligible corrosion was observed on all titanium specimens exposed. Welded specimens of vacuum-induction melted, low-carbon Ni-o-nel appeared to be free of localized attack in the heat-affected zone after 96 hr exposure to Thorex dissolver solutions. Titanium in 0.5 M HBF_4-HNO_3 corroded at maximum rates varying from 19 mils/mo in 3 M HNO_3 in the presence of dissolving zirconium to 295 mils/mo in 12 M HNO_3 with no zirconium present. Preferential edge attack of Haynes experimental alloys EB4358 and EB5459 in boiling Sulfex solution was eliminated by smoothing the cut edges of the specimens. Random pitting was not eliminated. Preliminary tests of titanium-45A in HNO_3-0.5 M $Fe(NO_3)_3$ solutions for U-Mo core dissolution showed rates $\leq$0.24 mil/mo for 72 hr exposures in the range of 3-8 M HNO_3 but results were erratic and some localized attack was observed.

Mechanisms of Separation Methods

Radiation Damage to Solvents and Diluents. A procedure is being developed to analyze for di-monobutyl and ortho phosphoric acids in solutions containing TBP, Amsco 125-82, nitric acid, and water. The method involves separating the acids from each other and from other solution components by ascending

paper chromatography, cutting the paper into short sections, irradiating these sections in a neutron flux of ~10^{13} n/cm^2·sec for 1 hr, and finally beta counting of the P-32 formed by the neutron activation. Accuracies are of the order of ±20% when the phosphorus content of an individual acidic phosphate is down to ~0.02 g/liter of solution.

Solubility of Ferric Mono- and Dibutyl Phosphates in Process Solutions. Ferric mono- and dibutyl phosphates were prepared in pure form for use in measuring their solubilities in aqueous nitric acid and 30% TBP-Amsco-HNO_3 solutions. Solubilities of $Fe_2(MBP)_3$ in the aqueous phases increased from 1.8×10^{-4} to 8×10^{-2} M and in the organic phases from $<1.4 \times 10^{-4}$ to 3.4×10^{-2} M as the nitric acid in the aqueous phases increased from 0 to 2.96 M, corresponding to 0 to 0.64 M HNO_3 in the organic phases. Solubilities of $Fe(DBP)_3$ were below the spectrographic limit of detectability, ~1×10^{-5} M, in the organic phases and increased from $<1 \times 10^{-5}$ to ~4×10^{-4} M as the acidity in the aqueous phases increased from 0 to 3.2 M.

Waste Treatment

A synthetic Purex 1WW waste concentrate, with 1.2 mol/liter Na and 0.2 mol/liter Mg added to reduce sulfate volatility, was calcined to 900°C semi-continuously in a 4 x 18 in. stainless steel pot. The solid residue had a volume equivalent to about 6 gal per ton of U processed, a density of about 1.32 g/ml, a porosity of about 58%, a thermal conductivity of 0.155 Btu/hr-ft-°F at 475°F, and a thermal conductivity of 0.207 and 676°F. The condensate and off-gas scrubber contained 0.28% and 0.02% of the feed sulfate, respectively. A closed system was used, with gas recirculation, and nitric oxide was added as required to keep the system pressure near atmospheric. This method of operation resulted in approximately zero net noncondensible off-gas production for the run.

In small-scale evaporation-calcination experiments in glass equipment with a nitric oxide sweep gas, the ruthenium volatility was 1.5-32.6%, depending on the amount and kind of additives. In earlier similar runs without nitric oxide the ruthenium volatility was almost 80%.

In studies of the decontamination of ORNL process water waste the presence of 10 ppm EDTA was found to have negligible effect on the performance of Duolite C-3 phenolic resin. Duolite CS-100 phenolic-carboxylic resin was found to regenerate with 1 M HCl about as efficiently as Duolite C-3 phenolic-sulfonic resin did with 5 M HCl on a volume basis, i.e., 99.9+%, regeneration is achieved with about ten resin volumes in either case.

Ion Exchange

A corrected calculation of fission product concentrations expected in Purex 1WW waste from Processing Yankee Atomic Reactor fuel was made. To simulate low-burnup processing wastes a synthetic 1WW solution was made up using 10% of the fission product concentrations calculated for Yankee conditions using stable isotopes for the fission products. The simulated

1WW contained 0.185 g Sr and 1.6 g rare earths per liter. After 10X dilution and adjustment to 0.124 M in oxalic acid the solution was passed through Dowex-50W resin until the 50%-breakthrough for rare earths, as indicated by Ce-Pr-Eu-Y tracers, was reached at about 74 resin volumes. About 99.8% of the rare earths were eluted from the resin with 25 resin volumes of 0.5 M monosodium citrate (pH 3.5).

Chemical Applications of Nuclear Explosions (CANE)

Tritium exchange from the water form to molecular hydrogen was .07%/g $CaSO_4$ at 380°C and 2.7%/g of $CaSO_4$ at 700°C when a flow ratio of hydrogen to water vapor of 20 was used in 40 min determinations. The exchange rate reaches a maximum 50 min after increasing according to a parabolic equation which indicates the rate is controlled by bed diffusion. Under static conditions, the rate of reduction of $CaSO_4$ by hydrogen was virtually independent of hydrogen pressure in the 200-500 mm range at 700°C. The mechanism of the reaction is not known at present. The reduction rates at constant volume were 0.14 and 0.12 mm of hydrogen/m^2·min for samples having surface areas of 2.9 and 0.82 m^2/g, respectively. Calcium sulfate is readily decomposed when fine powders of $CaSO_4 \cdot 1/2\ H_2O$ are sprayed into a plasma jet. Thermal decomposition of ammonium bicarbonate is probably too slow to permit its use as a "filler" for the Gnome sample pipe. Approximately 20 min were required to decompose 10 g of the material at temperatures in the 100-200°C range. Ammonium dicarbonate was melted when heated in scaled glass tubes at 130°C.

CONTENTS

1.0 POWER REACTOR FUEL PROCESSING

1.1 Dissolution Studies (L. M. Ferris)

1.1.1 Dissolution of Consolidated Edison Fuel (A. H. Kibbey)

In the continuing study of the dissolution of high density ThO_2-UO_2 fuel pellets, the effect of having boron or cadmium in the dissolvent, 13 M HNO_3--0.04 M NaF--0 to 0.1 M $Al(NO_3)_3$, was partially evaluated. Boron and cadmium are being considered as soluble neutron poisons to aid in criticality control during fuel dissolution.

The pellets used in these studies were supplied by the Universal Match Company and contained 5.3% $UO_{2.0}$. The geometric densities varied from 92 to 94% of theoretical. In three series of experiments, made to evaluate the effect of boron, initial 10-min rates of dissolution were determined in boiling 13 M HNO_3--0.04 M NaF containing 0, 0.04, and 0.1 M $Al(NO_3)_3$ and boric acid in concentrations up to 0.2 M. A 200% stoichiometric excess of dissolvent was used in each case. The highest 10-min rate, about 2 mg $min^{-1}cm^{-2}$, was obtained when the dissolvent contained no aluminum and less than 0.1 M H_3BO_3. When the boric acid concentration was constant, the 10-min rate decreased with increasing aluminum concentration as expected[1] (Fig. 1). In each series at constant aluminum concentration, the 10-min rate was independent of boric acid concentration up to 0.1 M; however, the rate in solutions containing no aluminum or 0.1 M aluminum decreased about 30% as the boric acid concentration increased from 0.1 to 0.2 M. The rate in all solutions containing 0.04 M aluminum was nearly constant at 1.3 mg $min^{-1}cm^{-2}$.

Systems containing boron require further investigation since, in one attempt to produce a 1 M thorium solution by dissolution of the pellets in 13 M HNO_3--0.04 M NaF--0.1 M $Al(NO_3)_3$--0.1 M H_3BO_3, about 25% of the thorium precipitated as $Th(NO_3)_4$. Furthermore, only 98.8% of the pellets dissolved in 75 hr compared to complete dissolution in 60 hr of a similar batch of pellets in 13 M HNO_3--0.04 M NaF--0.1 M $Al(NO_3)_3$--0.025 M $Cd(NO_3)_2$. No precipitation was observed in the solution containing cadmium.

Cadmium produced a surprising effect on the initial 10-min rate of dissolution. In solutions containing no aluminum the rate decreased from 2 to 0.7 mg $min^{-1}cm^{-2}$ as the cadmium concentration increased from 0 to 0.075 M (Fig. 2). The opposite effect occurred with 0.1 M aluminum in the same solution, the rate increasing from 0.7 to 2 mg $min^{-1}cm^{-2}$ as the cadmium concentration increased from 0 to 0.075 M. Only a slight decrease in rate with increasing cadmium concentration was observed when the aluminum concentration in the dissolvent was 0.04 M. Since the reason for this behavior is not obvious, the experiments are being repeated to substantiate the results.

1.1.2 Dissolution of Uranium-Molybdenum Alloy Fuel (L. M. Ferris)

Scouting experiments were conducted to determine what solids were formed when U-10% Mo alloy was dissolved in boiling nitric acid. Pieces of the alloy were dissolved in boiling nitric acid (initially 5, 8 and 11 M)

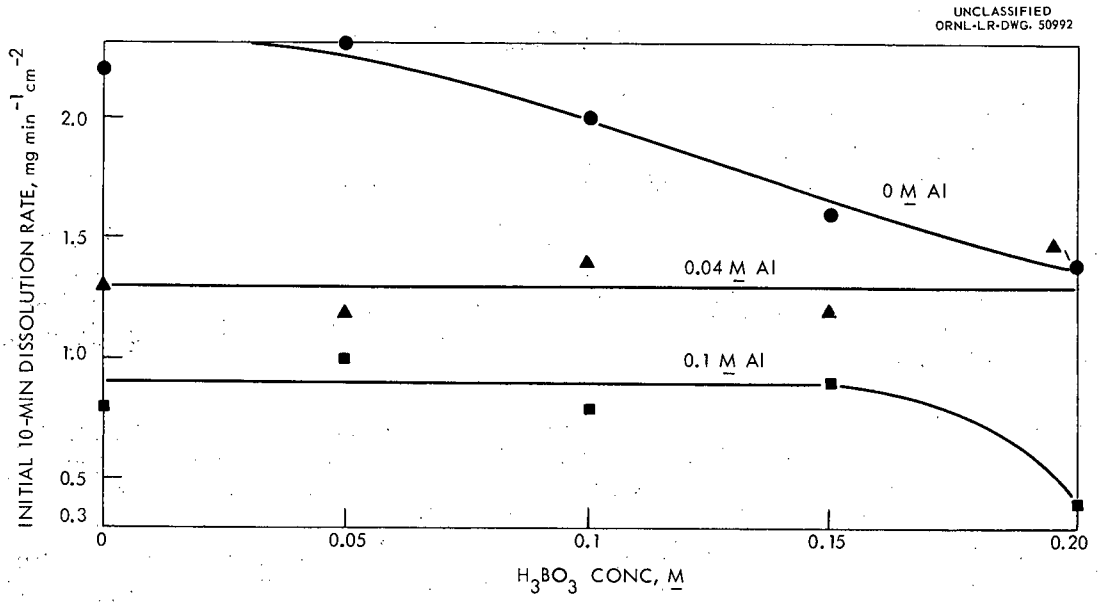

Fig. 1. Effect of boric acid and aluminum nitrate concentrations on the initial 10-min rate of dissolution of Universal Match Co. 94.7% ThO_2-5.3% UO_2 pellets in 200% stoichiometric excess of boiling 13 M HNO_3-0.04 M NaF. Pellet densities: 92-94% of theoretical.

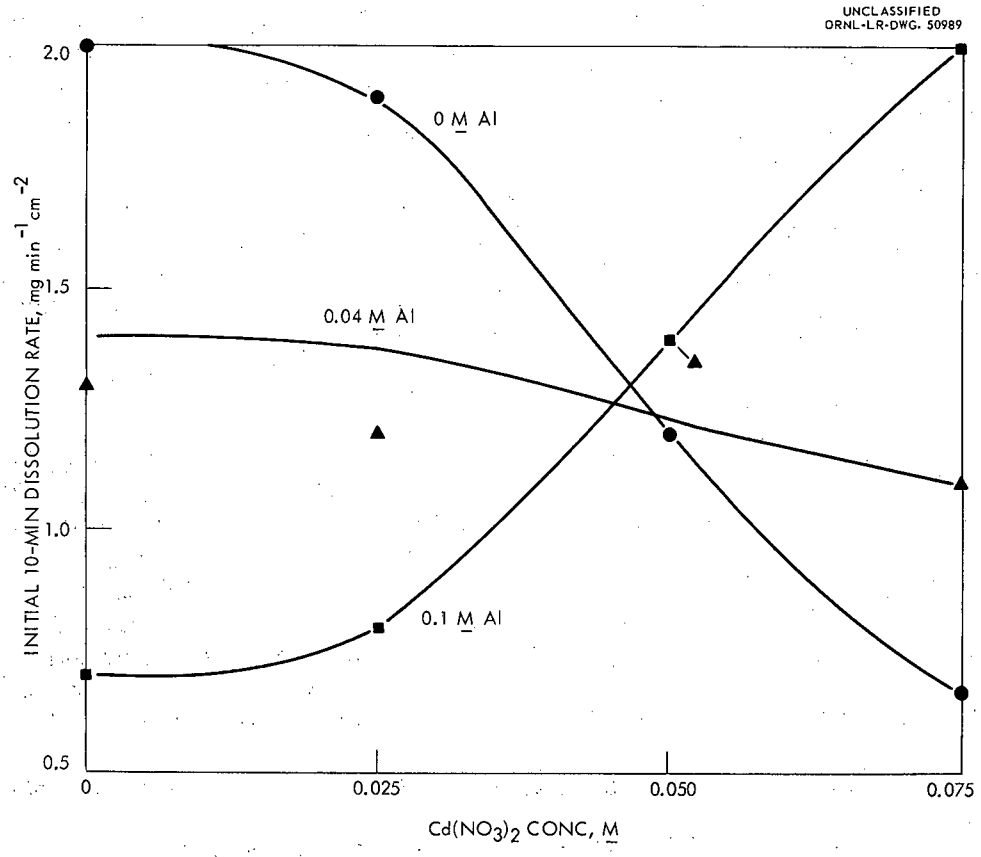

Fig. 2. Effect of cadmium nitrate and aluminum nitrate concentrations on the initial 10-min rate of dissolution of Universal Match Co. 94.7% ThO_2-5.3% UO_2 pellets in 200% stoichiometric excess of boiling 13 M HNO_3-0.04 M NaF. Pellet densities: 93-94% of theoretical.

to produce solutions containing about 1 M uranium. In each case solids formed shortly after dissolution began. In agreement with HAPO observations,[2] the Mo/U mole ratio in the solids increased sharply with increasing acid concentration (Table 1). Apparently, a series of uranyl molybdates is formed in which the uranium content steadily decreases with increasing acidity. For example, the normal molybdate, UO_2MoO_4, has been prepared by mixing unacidified uranyl nitrate and sodium molybdate solutions and $UO_3 \cdot 2MoO_3$ from similar mixtures containing 1 to 2 M HNO_3. In solutions of high acid concentration only MoO_3 precipitates.

The tentative flowsheet[3] for U-10% Mo alloy fuels involves dissolution in 11 to 13 M HNO_3. The conditions are such that only MoO_3 should precipitate. A small amount of uranium (1-5%) may be associated with the solids but it is probably sorbed since the x-ray pattern of these solids showed only MoO_3 (Table 1). Washing with water or dilute acid should result in recovery of the sorbed uranium with little attendant dissolution of the MoO_3. When a uranyl molybdate is inadvertently precipitated, nitric acid in concentrations greater than 5 M will probably be required if a uranium-molybdenum separation is desired. This point is illustrated by the solubility behavior of UO_2MoO_4 in dilute nitric acid (Fig. 3). Equilibrating solid UO_2MoO_4 with nitric acid less concentrated than about 2 M resulted in solubilization of nearly equimolar amounts of uranium and molybdenum. At higher acid concentrations, the uranium solubility apparently continues to increase but the molybdenum solubility decreases as the solid phase is converted to MoO_3.

Table 1. Solids Formed When U-10% Mo Alloy is Dissolved in Boiling Nitric Acid

Run No.	HNO_3 Conc., M		U Conc., M	Solids			Mo/U Mole Ratio
	Initial	Final		x-ray	U,%	Mo,%	
1	5	0.80	0.94	-	40.0	38.5	2.4
2	8	3.20	1.05	-	5.05	55.6	27
3	11	5.50	1.11	MoO_3	0.21	61.5	727

1.1.3 Effect of Air and Irradiation on Uranium and Thorium Losses During Decladding of Consolidated Edison Fuel (T. A. Gens)

Experiments performed in the hot-cells indicated that the presence of air caused larger uranium and thorium losses during decladding of stainless steel clad uranium oxide fuels than did the presence of radiation.[4] This observation was confirmed in laboratory experiments with nonirradiated Consolidated Edison pellets.

Consolidated Edison pellets (93% of theoretical density, O/U ratio = 2.4) were placed in refluxing initial and final Sulfex and Darex solutions and the solutions were sampled periodically and analyzed to determine the percent uranium and thorium dissolved. In a duplicate set of experiments, air was

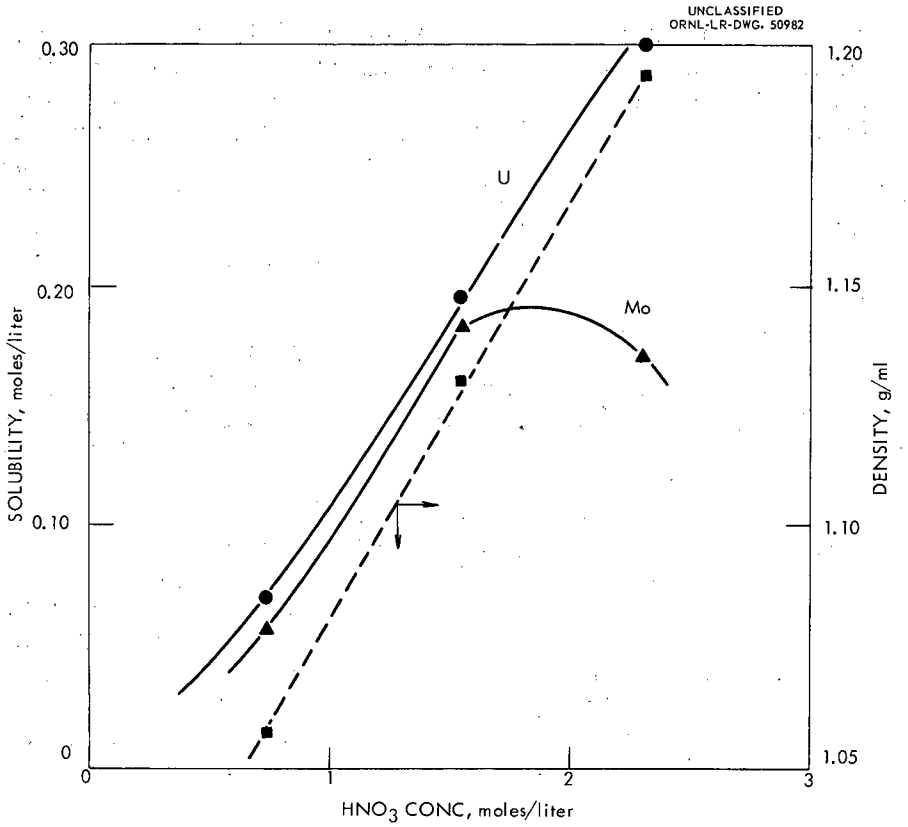

Fig. 3. Solubility at 26°C of UO_2MoO_4 in dilute nitric acid. Solid phase initially was UO_2MoO_4 in all cases.

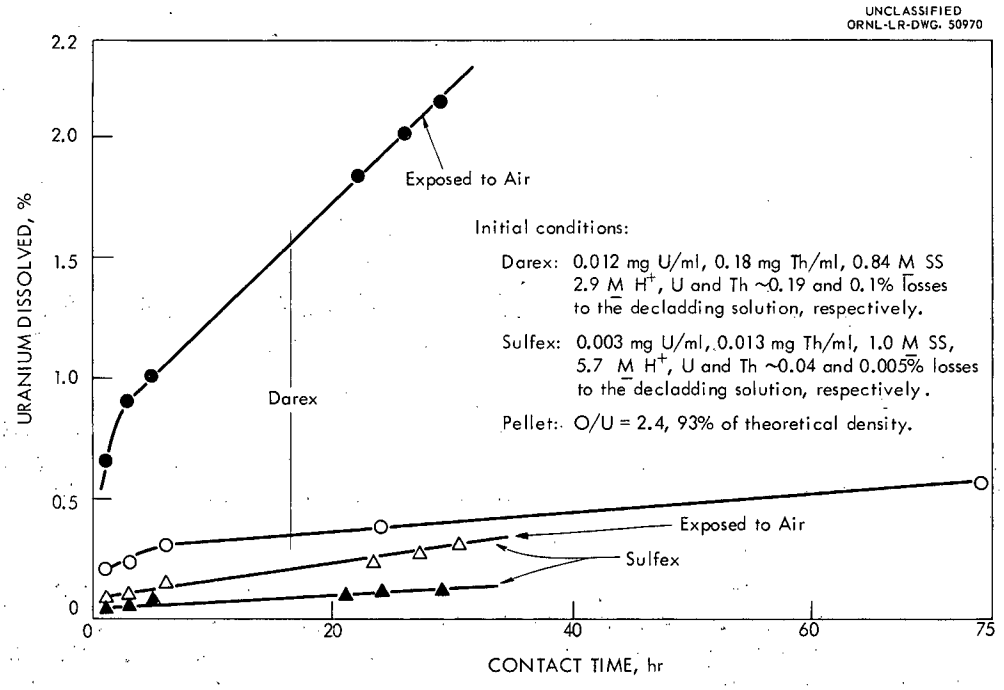

Fig. 4. Uranium losses from Consolidated Edison pellets to refluxing Sulfex and Darex solutions.

excluded by attaching a 6-ft plastic tube to the short (3-in.) water-cooled condenser. In another set of experiments with the plastic tube attached, the final solutions were exposed to Co^{60} radiation at a radiant power density of about 1 watt/liter. The losses observed in these experiments may be higher than will be found with the Consolidated Edison fuel because the Davison Chemical Company pellets used, although 93% of theoretical density, were less refractory in laboratory experiments than actual Consolidated Edison pellets. The final Sulfex and Darex solutions were prepared by decladding prototype Consolidated Edison fuel according to the respective flowsheets.[5]

Exposure of refluxing final decladding solutions to air (no irradiation) while contacting the Consolidated Edison pellets caused the Darex and Sulfex uranium losses to more than triple and double, respectively, at 3-hr contact time, and to increase at about 0.05 and 0.01%/hr, respectively, after 3 hr (Fig. 4). A similar, but somewhat smaller effect, was observed on thorium losses in refluxing final Darex solution, the thorium losses being almost too small to measure in refluxing final Sulfex solution (Fig. 5). Exclusion of air is particularly important in Darex decladding.

In practice, the average composition of the decladding solution contacting the core will lie between the initial and final solutions, and it was necessary to determine if large uranium and thorium losses occur during contact with the initial decladding solutions. Losses for the first 20 hr with air excluded were smaller in the initial Darex (Fig. 6) and Sulfex (Fig. 7) solutions than in the final solutions and increased rapidly when the initial solutions were exposed to air. In refluxing initial Darex solution, uranium losses increased at approximately 0.1% per hr and increased further to about 0.2% per hr when the solution was exposed to air (Fig. 6). Thorium losses followed uranium losses closely but were slightly smaller.

In refluxing initial Sulfex solution not exposed to air, uranium losses were only 0.02% in 3 hr and increased less than 0.01% per hr thereafter (Fig. 7). Exposure to air increased the uranium loss to 0.3% in 3 hr. The rate of increase after 3 hr was only 0.01% per hr. Air apparently causes a 3-fold larger increase in uranium losses for the first 3 hr in the initial than in the final Sulfex solution (see Fig. 4). The soluble thorium losses in initial Sulfex solution were limited to less than 0.2% by formation of insoluble thorium sulfate. However, exposure of the refluxing solution to air decreased the time needed to reach the maximum thorium concentration in solution from 20 to 3 hr.

Irradiation with Co^{60} radiation at a radiant power density of about 1 watt per liter, which is approximately the density expected in actual processing,[6] produced no measurable change in the uranium losses to refluxing final Darex solution over 70 hr (Fig. 8). Thorium losses for the first 3 hr were not increased by the irradiation, but appeared to be increased slightly after 3 hr. In the refluxing final Sulfex solution, similar irradiation appeared to cause about a 20% increase in uranium losses in 3 hr and had little effect thereafter (Fig. 9). No significant change in thorium losses was observed during irradiation of final Sulfex solution.

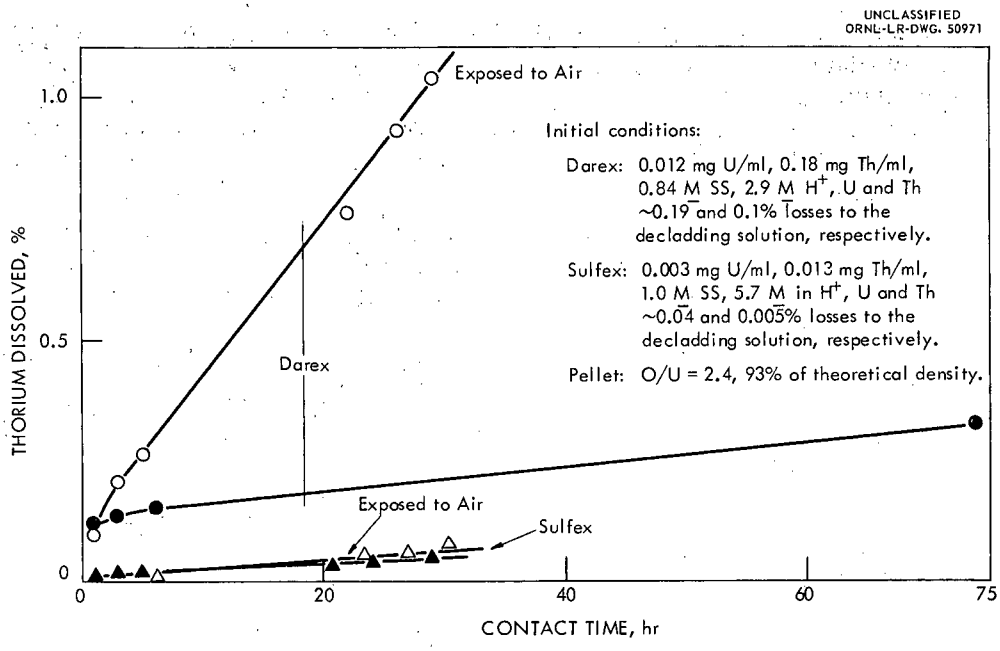

Fig. 5. Thorium losses from Consolidated Edison pellets to refluxing final Sulfex and Darex solutions.

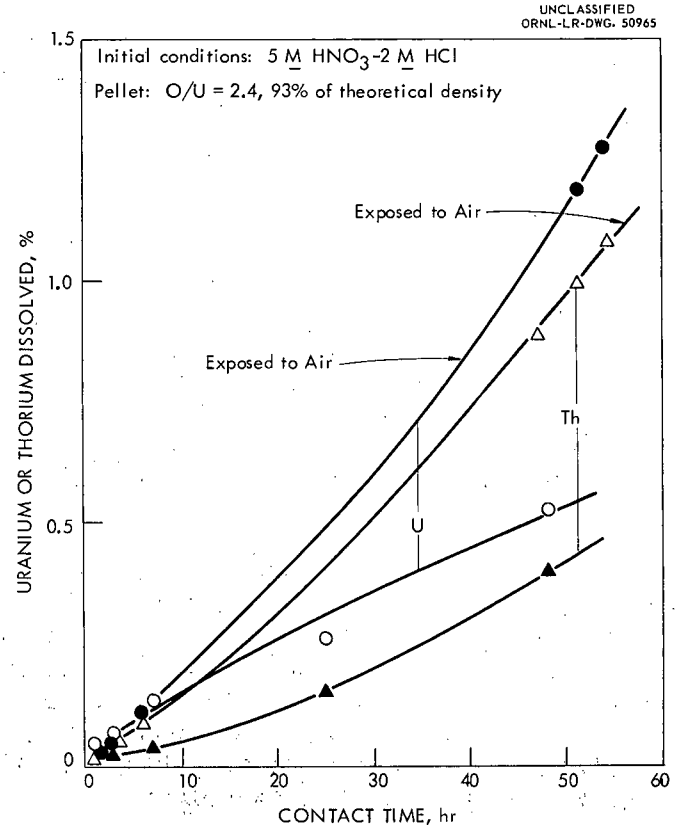

Fig. 6. Uranium and thorium losses from Consolidated Edison pellets to refluxing Darex solution.

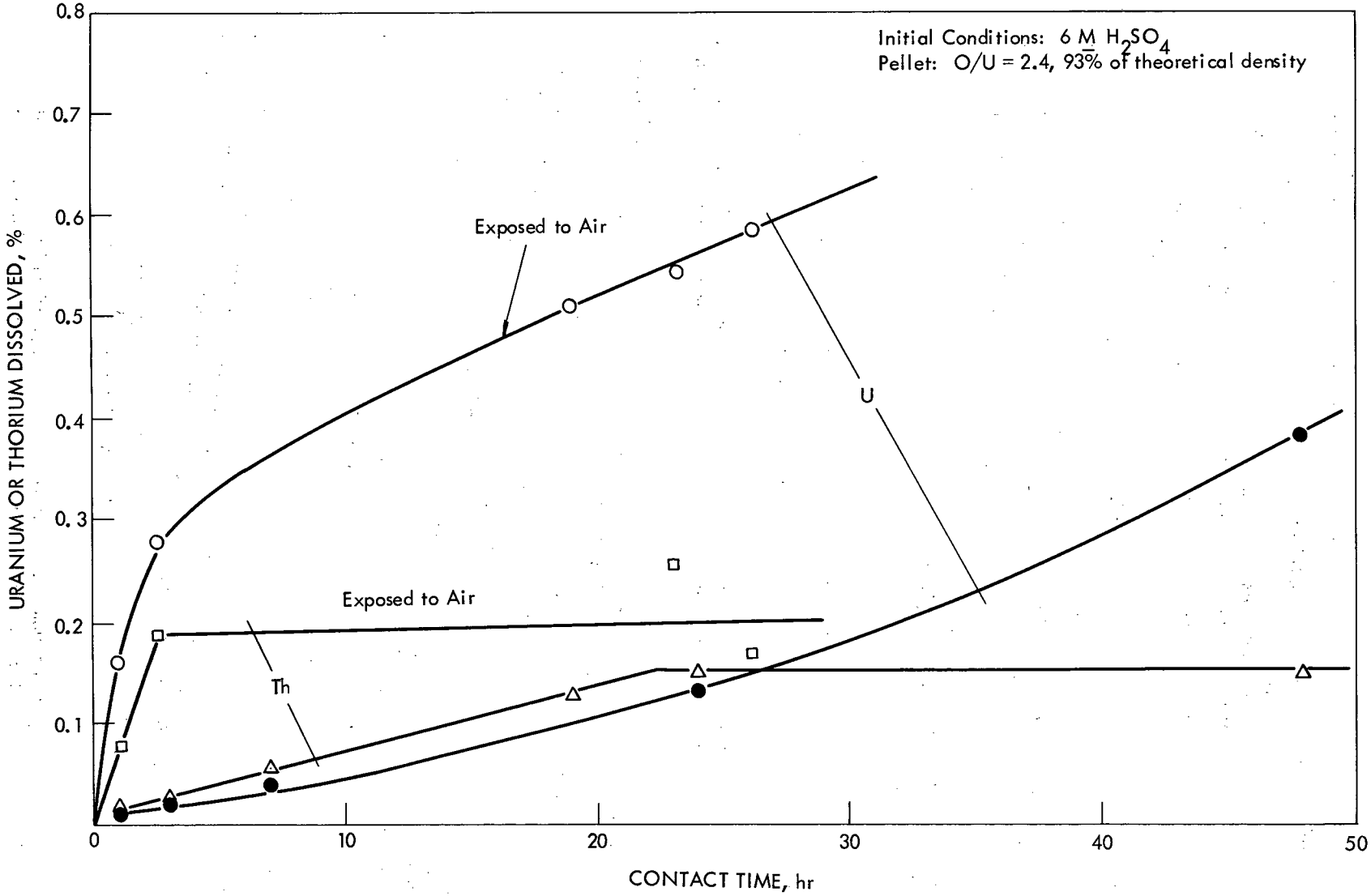

Fig. 7. Uranium and thorium losses from Consolidated Edison pellets to refluxing Sulfex solution.

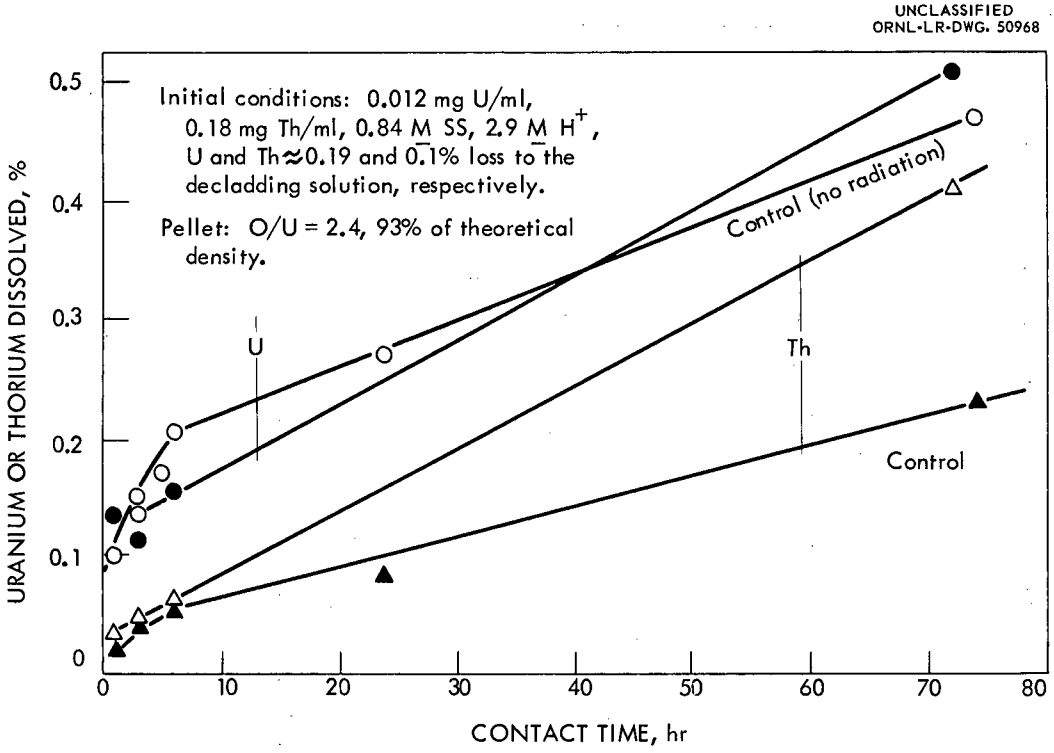

Fig. 8. Uranium and thorium losses from hydrogen-fired Consolidated Edison pellets to refluxing Darex solution in absence of air. Radiant Co-60 power density: 1 watt/liter.

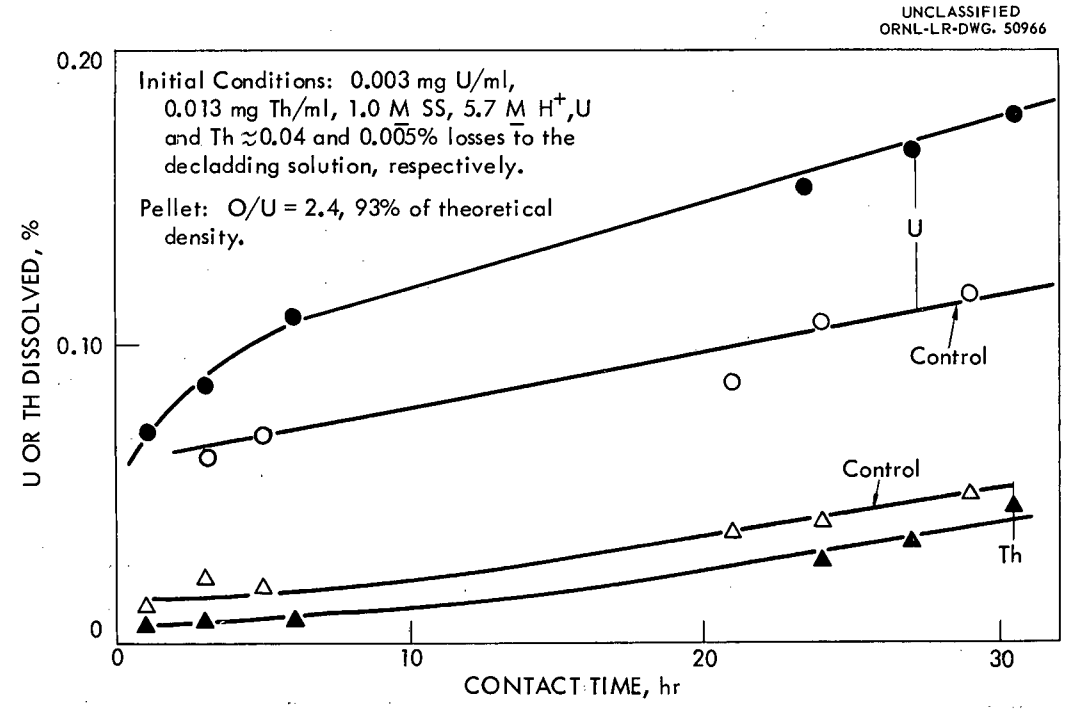

Fig. 9. Uranium and thorium losses from hydrogen-fired Consolidated Edison pellets to refluxing Sulfex solution in absence of air. Radiant power Co-60 density: 1 watt/liter.

1.1.4 Processing U-Mo Fuel by the Zircex Process (T. A. Gens)

Chlorination and hydrochlorination processing are being investigated as methods for processing U-Mo fuels as exemplified by the PRDC Blanket (U-3% Mo) and CPPD core (U-10% Mo). These techniques may have advantages over the presently proposed aqueous processes which have the disadvantage that they either produce large volumes of waste or require a solids-separation step.[7] Since these difficulties are more severe with high-molybdenum alloys, a 91.6% U-Mo alloy was used in this work. In the case of the stainless steel clad alloys, it was assumed that the clad will be removed by mechanical means and the uranium-molybdenum alloys will be recanned in aluminum, after destroying the sodium bonding material. An exception is the PRDC core alloy, whose zirconium clad can be removed by techniques developed in the Zircex process.[8,9,10] The reaction of uranium-molybdenum alloys with hydrogen chloride has been observed previously.[8]

Preliminary studies indicate that either chlorination or oxyhydrochlorination processes are feasible, with satisfactory reaction rates and molybdenum separations being achieved in both cases. Molybdenum separation occurs through volatilization of molybdenum pentachloride or oxychloride and formation of relatively nonvolatile uranium chloride or oxide during chlorination or treatment with hydrogen chloride-air mixtures, respectively. Chlorination offers the advantage of nearly quantitative volatilization of molybdenum compounds but also causes volatilization of some uranium chloride. Treatment with hydrogen chloride-air mixtures permits rapid reaction at moderate temperatures, smaller amounts of chloride waste, and probably lower corrosion rates, but removes only 90% of the molybdenum. Removal of the aluminum jacket may be accomplished by either chlorination or hydrochlorination to form volatile aluminum chloride. Removal of the original stainless steel clad and destruction of the sodium bond by chlorination may also be possible.

The reaction rate of hydrogen chloride-air mixtures with 91.6% U-Mo alloy in 1-hr runs at 500°C increased from about 3.5 mg/cm^2-min in pure hydrogen chloride to about 8 mg/cm^2-min in 10-90% HCl-air mixtures (Fig. 10). The amount of molybdenum removed, as volatile molybdenum oxychloride (vapor pressure = 1 atm at ~100°C), exceeded 80% when the air content of a hydrogen chloride-air mixture exceeded 50% (Fig. 10). Apparently a temperature of 400°C with 10% HCl-air produces a reaction rate and molybdenum removal approximately equal to that achieved at higher temperatures (Fig. 11).

While the reaction rates shown in Figs. 10 and 11 are moderately high, ~8 mg/cm^2-min, the large diameters of the fuels under consideration, 0.415 and 0.59 in. for the PRDC blanket and the CPPD, fuel, respectively, would require processing times of 20 hr or longer. Only about 7 hr would be required for the 0.148 in. PRDC core, clad in 5 mils of zirconium. Experiments lasting 2 and 3 hr at 400°C in 10-20% HCl-air produced rates equal to those observed in 1-hr studies, within the expected experimental precision, indicating that the rate is independent of the amount of alloy which has reacted. Longer experiments are planned. The amount of molybdenum and chloride removed from the product increased from 74 to 86% and 99.3 to 99.7%, respectively, as the reaction time increased from 1 to 3 hr. One-hour rate

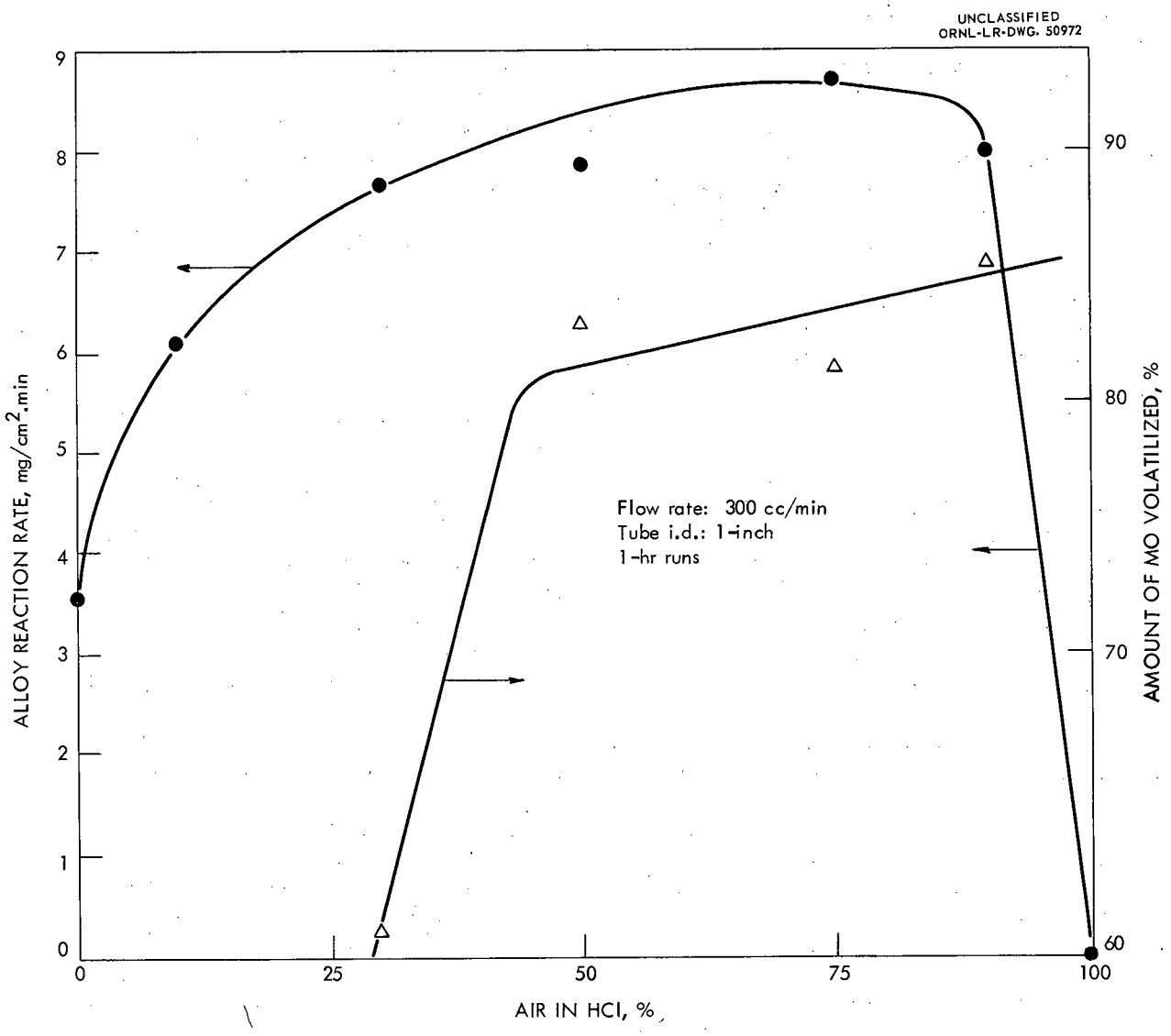

Fig. 10. Reaction rate of 91.6% U-Mo alloy with HCl-air mixtures at 500°C.

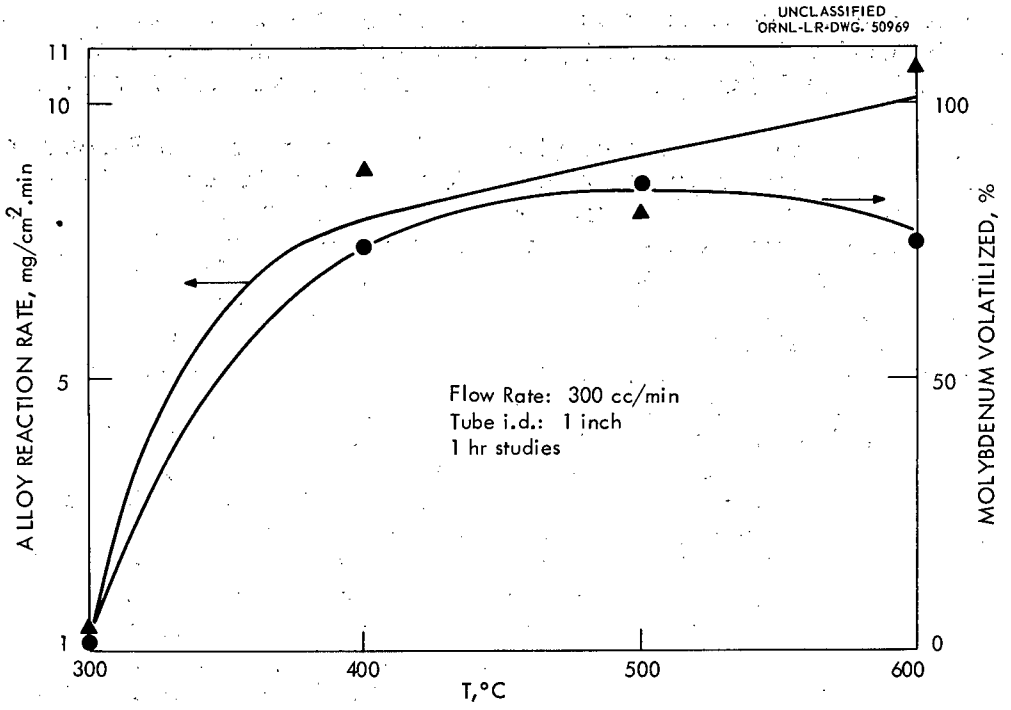

Fig. 11. Reaction rate of 91.6% U-Mo alloy with 10% HCl-90% air.

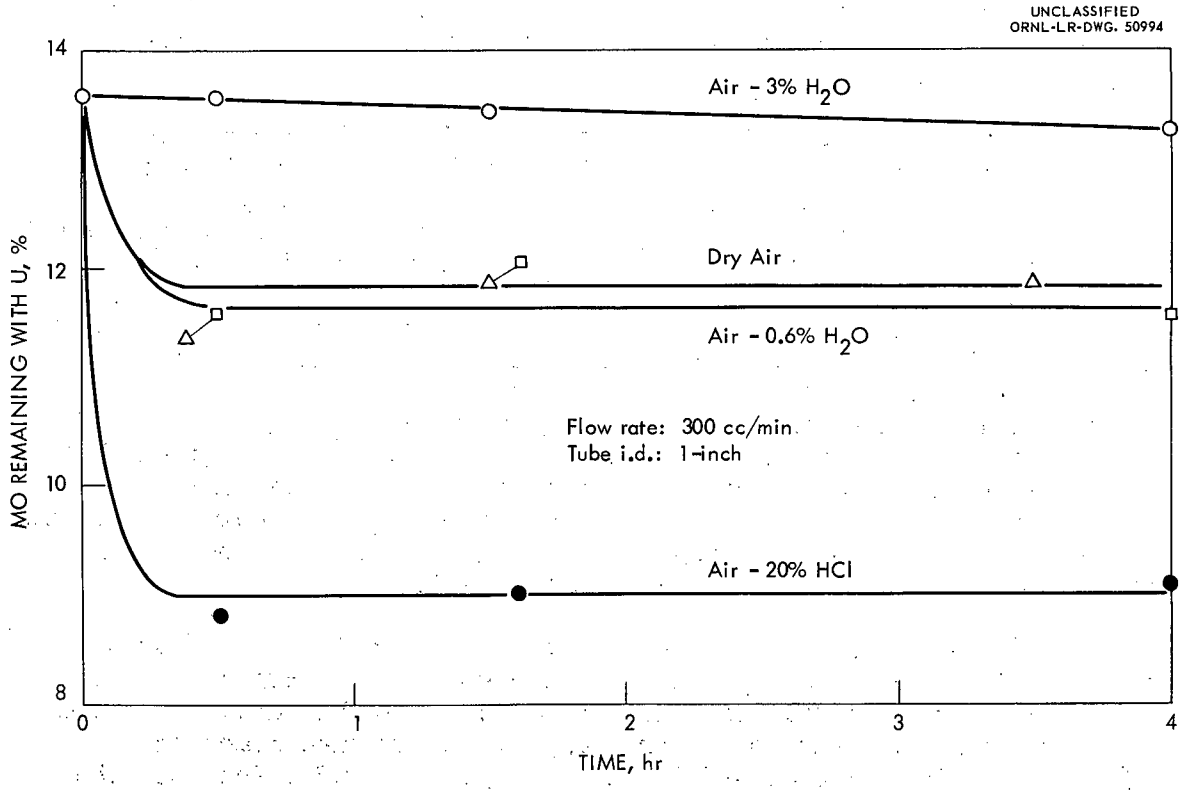

Fig. 12. Volatilization of molybdenum from product of 3-hr reaction of 91.6% U-Mo alloy with 10-20% HCl-air at 400°C.

studies showed higher reaction rates of 11-13 mg/cm^2-min at 400°C in 15% HCl-air with 3 and 10% Mo-U alloys. The higher rates are probably caused by different metallurgical histories and are being investigated further.

The product of the reaction of 91.6% U-Mo alloy with 10% HCl-air at temperatures above 400°C appears to be mostly uranium dioxide. Assuming that the product of hydrochlorination would be mostly uranium trichloride, the dilution with 90% air caused removal of over 99% of the chloride in 1-hr runs at reaction temperatures of 400°C or higher. At 400°C, the amount of chloride remaining in the product of a 1-hr run corresponded to 700 ppm chloride in a 1 M uranium solution. Further treatment at 400°C of the product from the 3-hr run discussed above showed that air containing 0.6% H_2O reduced the chloride content from 99.7% or 420 ppm in a 1 M U solution to 60 ppm and the molybdenum content from 13.6% to 11.6% in 4 hr. It should be possible to reduce the chloride concentration sufficiently that a Darex chloride removal step[10,11] will not be necessary before solvent extraction in stainless steel equipment. While air containing 0.6% H_2O was more effective in removing chloride than dry air, air-3% H_2O or air-20% HCl, air-20% HCl was more effective in removing molybdenum, apparently approaching a limiting value of 91% removal within 0.5 hr (Fig. 12). Since the processing time using 10-20% HCl-air might be as long, as 25 hr, the molybdenum content of the product should approach closely the limiting value of 91% removal, without additional treatment.

When using 10% HCl-air, the calculated maximum hydrogen concentration which could be produced in the off-gas by 100% utilization of the hydrogen chloride is 5%. However, water appears as a major product at a reaction temperature of 400°C.

The reaction rate of the 91.6% U-Mo alloy with chlorine was very low below a furnace temperature of 400°C but increased rapidly to 20 mg/cm^2-min as the furnace temperature increased from 425°C to 450°C or higher. The highly exothermic reaction caused the temperature of the alloy to increase rapidly to red heat. A volatilization of 87-98% of the molybdenum, as molybdenum pentachloride (vapor pressure = 1 atm at 268°C), was achieved in the 400-500°C temperature range. This exceeded the approximately 85% volatilized in 1 hr at 500°C with HCl-air mixtures, probably because a nonvolatile molybdenum oxide was produced by the latter reagent. The amount of uranium chloride volatilized was not measured in these experiments, but analyses of the product residues from reaction with HCl-air indicated that no uranium was lost. Visual observation indicated uranium chloride was volatilized when chlorine was used as the reagent at 500°C. Volatile uranium chloride can probably be selectively condensed by techniques developed in the Zircex process,[9] particularly when using HCl-air.

Attempts to use mixed chlorine-air were not successful. The stronger oxidizing conditions produced by Cl_2-air, as contrasted to HCl-air, caused formation of a protective coat of yellow material, possibly uranyl chloride, which inhibited further reaction. For example, the average reaction rate of 91.6% U-Mo in 1-hr tests at 425°C fell from 3.2 to 0.27 mg/cm^2-min when

chlorine was diluted with 25% air.

Phosgene, which resembles hydrogen chloride in that the product of its reaction with uranium-molybdenum alloy contains a reducing gas (CO), reacted with 91.6% U-Mo at 500°C in a 0.5 hr run at a rate double that of HCl-air, when the phosgene was mixed with air. Much of the molybdenum and chloride, 39 and about 50%, respectively remained in the product. Pure phosgene produced very little reaction. Addition of phosgene to HCl-air mixtures caused the reaction rate to decrease.

Initial studies indicate that the aluminum jacket in which the fuel will be received can be removed by reaction with either hydrogen chloride or chlorine at furnace temperatures as low as 300°C (Fig. 13), to form volatile aluminum chloride (vapor pressure = 1 atm at 183°C). A small amount of ammonium chloride is needed to initiate the reaction. Neither hydrogen chloride (Fig. 11) nor chlorine reacts rapidly with the 91.6% U-Mo alloy at 300°C. The reaction rate in 5-15 min studies of both gases with aluminum decreased approximately linearly from 11.4 mg/cm^2-min as they were diluted with nitrogen. The rate decrease with dilution is probably caused by a reduction in both the reagent concentration and the temperature of the aluminum. When reacting with pure hydrogen chloride or chlorine, the aluminum soon reached red heat and began to flow but did not melt (melting point of pure aluminum = 660°C). The reaction rate of 5.4 mg/cm^2-min observed when using 60% HCl-air, yields a 7-hr decanning time assuming the aluminum can is 32 mils thick.

Initiation periods for the reaction at 300°C between hydrogen chloride or chlorine and aluminum of between 3 and 9 min were observed, even with the use of ammonium chloride as an initiator, except in the case of chloride diluted with 85% nitrogen where the initiation period was 38 min (Fig. 13). Some unknown variable, perhaps a small amount of air or moisture in the reagents, caused the aluminum samples to be passive initially. For example, in 1 run at 300°C in pure chlorine without ammonium chloride as an initiator, no reaction occurred in 1 hr. In a duplicate run, reaction started within 30 min. In all cases in which ammonium chloride was added as initiator and the reagent gas was not diluted more than 50% with nitrogen, reaction started in less than 10 min at 300°C.

If high temperature chlorination or hydrochlorination could be used to remove the stainless steel clad from the original PRDC or CPPD fuels, the mechanical decladding operation might be avoided. Such a process offers the potential advantage that the sodium bonding material may be destroyed in a gas-solid reaction with the same reagent used for clad removal. Studies of the reaction rate of 304 SS with chlorine showed that a temperature of at least 600°C is required to achieve rates of over 0.5 mg/cm^2-min. A small amount of water vapor, not exceeding about 6%, increased the rate slightly. Although a light-yellow surface coat developed during chlorination, average reaction rates with pure chlorine at 600°C were the same in a 0.5 hr run as in a 2-hr run. The x-ray pattern of nickel chloride was observed from the material in the surface coat. The major chlorination product is

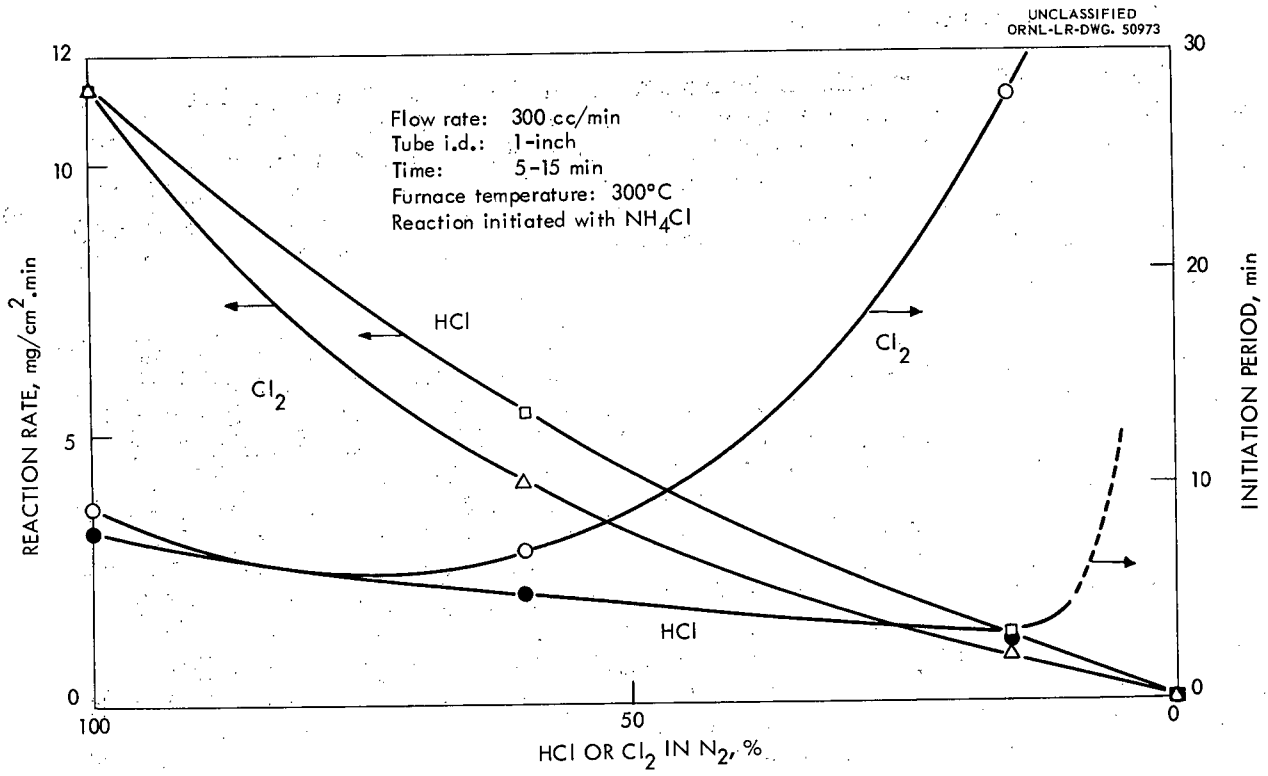

Fig. 13. Reaction rate of 2S aluminum with HCl or Cl_2-N_2 mixtures.

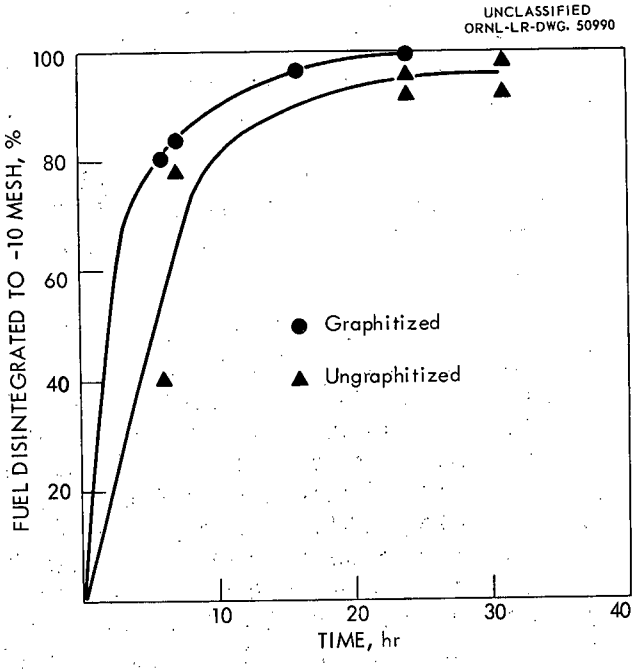

Fig. 14. Rate of disintegration of 1.5 in. dia prototype spheres of pebble bed reactor fuel (National Carbon) by 90% HNO_3.

thought to be ferric chloride (vapor pressure = 1 atm at 315°C). Chromium may be forming either the volatile chromic chloride hydrate (vapor pressure = 1 atm at 83°C) or chromyl chloride (vapor pressure = 1 atm at 118°C). The fuels under consideration have 10 mil stainless steel cladding, which would require 6 hr for complete reaction at a rate of 0.55 mg/cm^2-min. The chloride salts of sodium and nickel would have to be dissolved in water and removed prior to processing the core unless chloride is removed by techniques used in the Darex process.[10,11] Use of chlorine at 600°C would probably produce severe corrosion in most metallic materials of construction. Reaction rates of hydrogen chloride with 304 SS were about an order of magnitude lower than those of chlorine.

1.1.5 Recovery of Uranium from Graphite Fuels (M. J. Bradley)

Application of the grind-leach[12] and 90% HNO_3[13] methods to the recovery of uranium from several prototypes of Pebble Bed reactor fuel was studied briefly. Two of the fuel samples were 1.5 in. dia spheres weighing about 50 g and containing uranium incorporated by the admixture technique. These samples were baked at 1450°C, and half the batch was further heated to graphitize the binder and convert the uranium to UC_2 (vender National Carbon). The third sample consisted of UO_2 (100 to 200 μ) admixed with graphite and the binder; fuel baked, reimpregnated with binder, coated with an unfueled graphite shell 0.15 in. thick, and finally a Si-SiC layer, 0.003 in. thick (vender Minnesota Mining and Manufacturing Company). This piece was heated to 3600°F which converted the uranium to UC, but did not graphitize the binder. The specimen was broken during impact tests and the UC hydrolyzed prior to the chemical studies.

The graphitized balls disintegrated more rapidly in 90% HNO_3 than the ungraphitized (Fig. 14). This was not unexpected since the disintegration of the graphitized specimens probably proceeds through the formation of the nitric acid lamellar compound, while ungraphitized carbon does not form lamellar compounds. With both types of fuel the outer layer disintegrated much more rapidly than the central core, which had been subjected to higher pressure in the molding operation. For example, 84% of the graphitized specimen disintegrated in the first 7 hr, but an additional 17 hr was required to complete the process. There was some variation among the ungraphitized balls. On Run 6 (Table 2), complete disintegration to -4 mesh powder occurred in 24 hr, while in Run 5 about 7% of the sample was still intact after 32 hr. It was advantageous to separate the powder, core, and nitric acid solutions after 6-10 hr, and contact the core with fresh acid. When the disintegrated material was contacted with 90% nitric acid for 24 hr, the resulting powder was so fine that it formed a slurry which was difficult to filter (Table 2, Run 5). The core appeared to disintegrate more rapidly after the powder had been removed (Table 2, Run 6 vs Run 5). After washing the partially disintegrated material with water and filtering under vacuum, no further disintegration occurred when 90% HNO_3 was added in the second leach (Runs 1 and 4). The disintegration proceeded as readily at 25°C as at the reflux temperature.

Table 2. Recovery of Uranium with 90% HNO_3 from 1.5 in. dia Prototype Spheres of Pebble Bed Fuel (National Carbon)

Procedure: 1st disintegration, 150 ml of 90% HNO_3
2nd disintegration, 25 ml of 90% HNO_3 (undisintegrated portion only)
Washes, 100 ml
2nd Leach, 150 ml of 90% HNO_3, 4-hr contact

	Graphitized			Ungraphitized		
Run No.	1	2	3	4	5	6
Sphere No.	315	311	312	269	273	275
U Conc., %	8.7	9.0	9.3	8.8	9.2	8.5
Disintegration time, hr — 1st Leach	6	16	7	6	24	7
Disintegration time, hr — 2nd Leach	-	24	17	-	-	17
Temperature	reflux	25°C	25°C	reflux	reflux	25°C
% Disintegrated to -10 mesh	81	100	100	41	93	98
Wash Solution	H_2O	HNO_3	HNO_3	H_2O	H_2O	HNO_3
U Found, % — 1st disintegration	81.1[a]	59.5	50.4	47.5[a]	69.7	47.9
U Found, % — 2nd disintegration	-	2.2	11.3	-	-	13.0
U Found, % — 1st wash		22.2	14.8		-	17.3
U Found, % — 2nd wash		8.2	13.3		-	16.4
U Found, % — 3rd wash	1.9	-	4.3	0.1	-	3.6
U Found, % — 2nd leach + 1 water wash	4.2	7.6[b]	4.2	14.4	25.5[c]	1.3
U Found, % — graphite residue (powder)	0.5	0.1	1.6	0.4	0.7[d]	0.5
U Found, % — graphite residue (core)	12.3	-	-	37.6	4.0	-

[a] Plus 2 washes.

[b] 15.8 M HNO_3, reflux.

[c] Plus 2 additional washes.

[d] 8-hr leach.

In general, two leaches with 90% HNO_3 (one of which occurs simultaneously with the disintegration) and four washes with either water or 90% HNO_3 recovered 99% or more of the uranium in the powdered residue (Table 2), but only about 30% of the uranium in the undisintegrated core. Complete disintegration of the fuel specimen, either graphitized or ungraphitized is essential for satisfactory uranium recovery. Higher uranium recoveries are obtained when boiling acid is used in the second leach than 25°C acid (Runs 2 and 3). All leach solutions from boiling 90% acid were a deep, wine-red color. When leaching was conducted at 25°C, the graphitized fuel which contained carbide yielded a red solution, but the ungraphitized yielded the typical yellow, uranyl nitrate color.

Uranium recovery by the standard grind-leach method[12] using 15.8 M HNO_3 (70%) was slightly higher from the ungraphitized National Carbon fuel than from the graphitized (Table 3). In general the leaching behavior of the two specimens was quite similar except that leach solutions from the ungraphitized fuel were dark red, while from the graphitized fuel they were yellow.

Only 99% of the uranium in the Si-SiC coated type could be recovered by grinding to -200 mesh and leaching twice with 70% (15.8 M) HNO_3 or grinding to -4+8 mesh and leaching with 90% HNO_3 (white fuming) (Table 3). When 70% acid was used, uranium recoveries were lower with more coarsely ground fuel. The 90% acid caused no apparent disintegration of the ground fuel. Leach solutions with 70% acid were the typical yellow of uranyl nitrate in nitric acid; with 90% acid a rust color.

Table 3. Recovery of Uranium by the Grind-leach Method (70% HNO_3) from Pebble Bed Prototypes

Composition			Uranium Found, %			
U, %	Fe, %	Particle Size Mesh	1st HNO_3 Leach + 2 Water Washes	3rd Water Wash	2nd HNO_3 Leach + 1 Water Wash	Graphite Residue
			Graphitized, National Carbon			
8.7	0.03	-4+8	90.4	0.2	7.0	2.4
8.2	0.02	-16+30	98.9	0.1	0.6	0.5
8.8	0.18	-200	99.3	0.001	0.3	0.4
			Ungraphitized, National Carbon			
7.0	0.04	-4+8	96.0	0.06	1.6	2.4
7.0	0.05	-16+30	97.5	0.1	2.3	0.16
9.8	0.3	-200	98.8	0.2	1.0	0.09
			Si-SiC Coated, Ungraphitized, 3 M			
7.6	0.02	-4+8	95.0	0.1	2.9	1.9
6.5	0.03	-10+20	96.3	0.2	1.6	2.1
11.3	0.4	-200	97.8	0.02	1.0	1.2
7.9	-	-4+8	92.5[a]	0.8	5.9[a]	0.8[a]

[a] 90% HNO_3 Leach.

1.2 Solvent Extraction Studies (R. H. Rainey, J. G. Moore)

1.2.1 Effect of TBP Concentration and Saturation on Decontamination Factors

A series of countercurrent batch extraction experiments using 5 to 15% TBP and 68 to 61% uranium saturation at the feed plate resulted in fission product decontamination factors which decreased a factor of about two with increasing TBP concentration. An experiment using 2.8% TBP, however, with only 38% uranium saturation at the feed plate, resulted in decontamination factors about 5 less than a similar experiment using 5% TBP with 68% saturation (Table 4). The experimental conditions were determined by McCabe-Thiele diagrams using the distribution coefficients for 2.5% TBP previously reported[14] and for 5, 10 and 15% given in Tables 5, 6, and 7 and Figures 15, 16, and 17. Decontamination factors were then determined by countercurrent batch extraction experiments. The uranium in the feed solution was maintained at 23 g/l but the acid was adjusted so that the aqueous waste would be 4 M HNO_3. The volume of the feed was adjusted to give a constant saturation in the organic at the feed plate.

The pregnant solvent was scrubbed with three stages of 2 M HNO_3. The volume of the scrub was 1/5 the volume of the organic phase. Decontamination from thorium varied from 23 to 38 in the series of experiments. This variation was not consistent with TBP concentration, uranium saturation, or uranium extraction factor. The number of extraction stages required to give less than 0.1% uranium loss increased from 5 stages using 15% TBP to 9 stages using 2.8% TBP.

1.2.2 Effect of Irradiation of Aqueous Feed on Decontamination

The use of the Acid-Thorex flowsheet to process synthetic Consolidated Edison aqueous feed solutions (irradiated at 2.6 watts/liter in a 10,000 curie Co-60 irradiation source prior to extraction), resulted in decreased decontamination factors after 5 and 10 watt-hr per liter irradiations but increased decontaminations after 40 and 165 watt-hr per liter irradiations (Table 8).

This improvement in decontamination factors following irradiation to greater than 40 watt-hr per liter is contrary to previous results using the Acid Deficient Thorex flowsheet.[15]

A series of countercurrent batch experiments were made using the following conditions:

Feed: 275 g/l Th, 16 g/l U, 0.18 N AD, 1 volume, stage 1E
Scrub # 1: 0.01 M PO_4, 0.01 M $Fe(SO_3NH_2)_2$, 0.8 volume, stage 6S
Scrub # 2: 5.0 M HNO_3, 0.2 volume, stage 3S
Acid: 13 M HNO_3, 0.5 volume, stage 4E
Solvent: 30% TBP-Amsco, 7 volumes, stage 5E
Stages: 5 extraction, 6 scrub

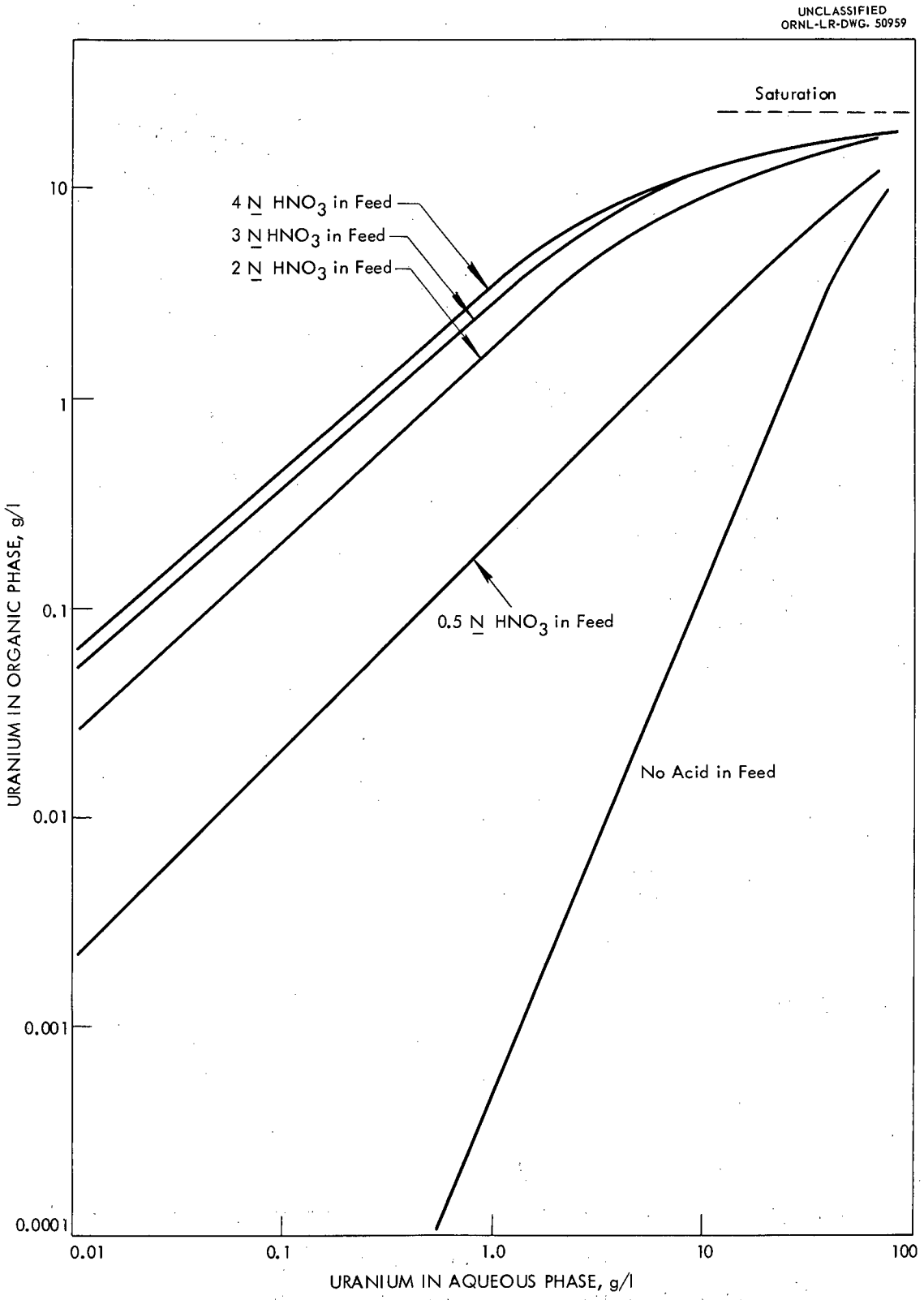

Fig. 15. Distribution of uranium between 5% TBP-Amsco and nitric acid solutions.

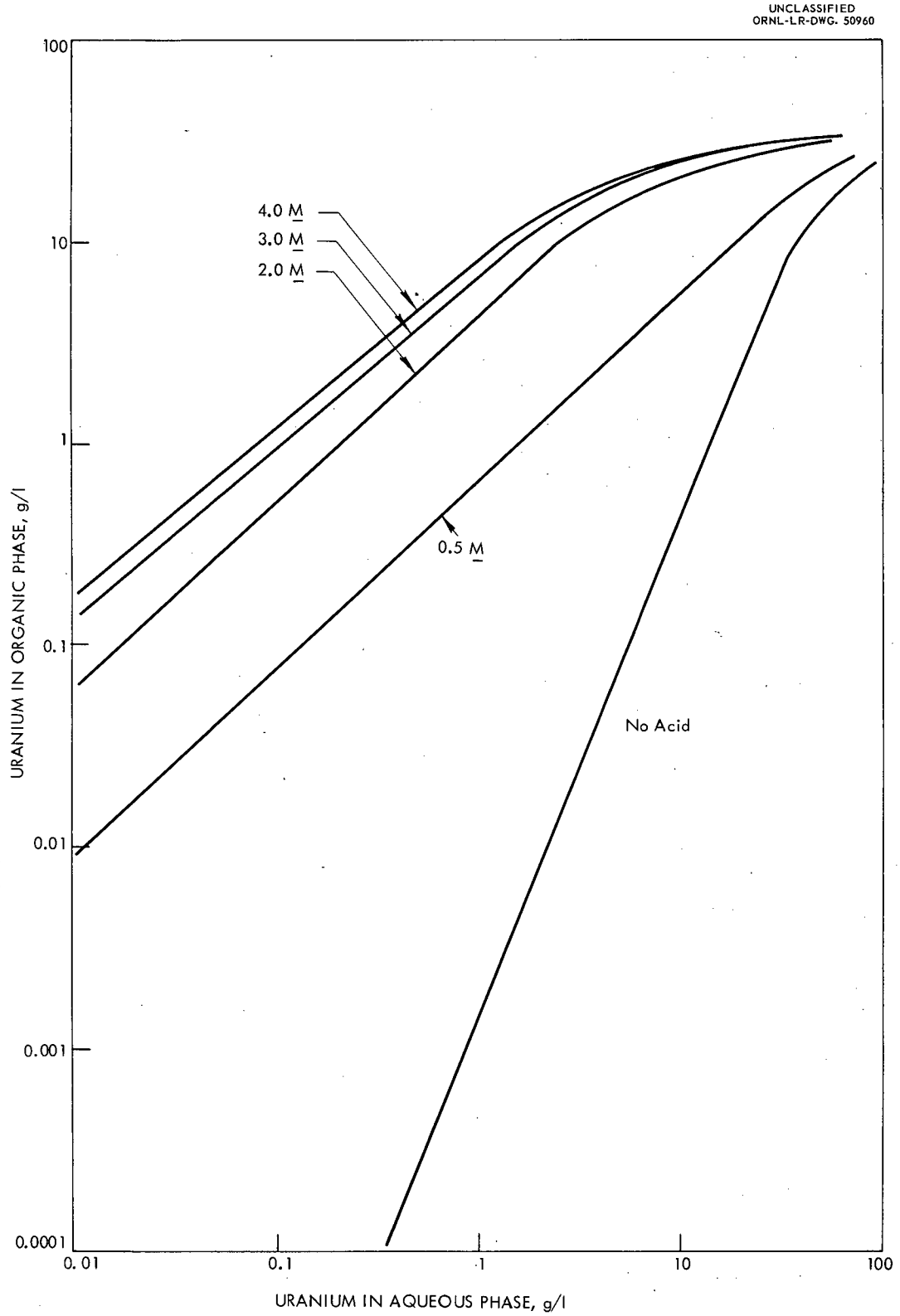

Fig. 16. Distribution of uranium between 10% TBP Amsco and nitric acid solutions.

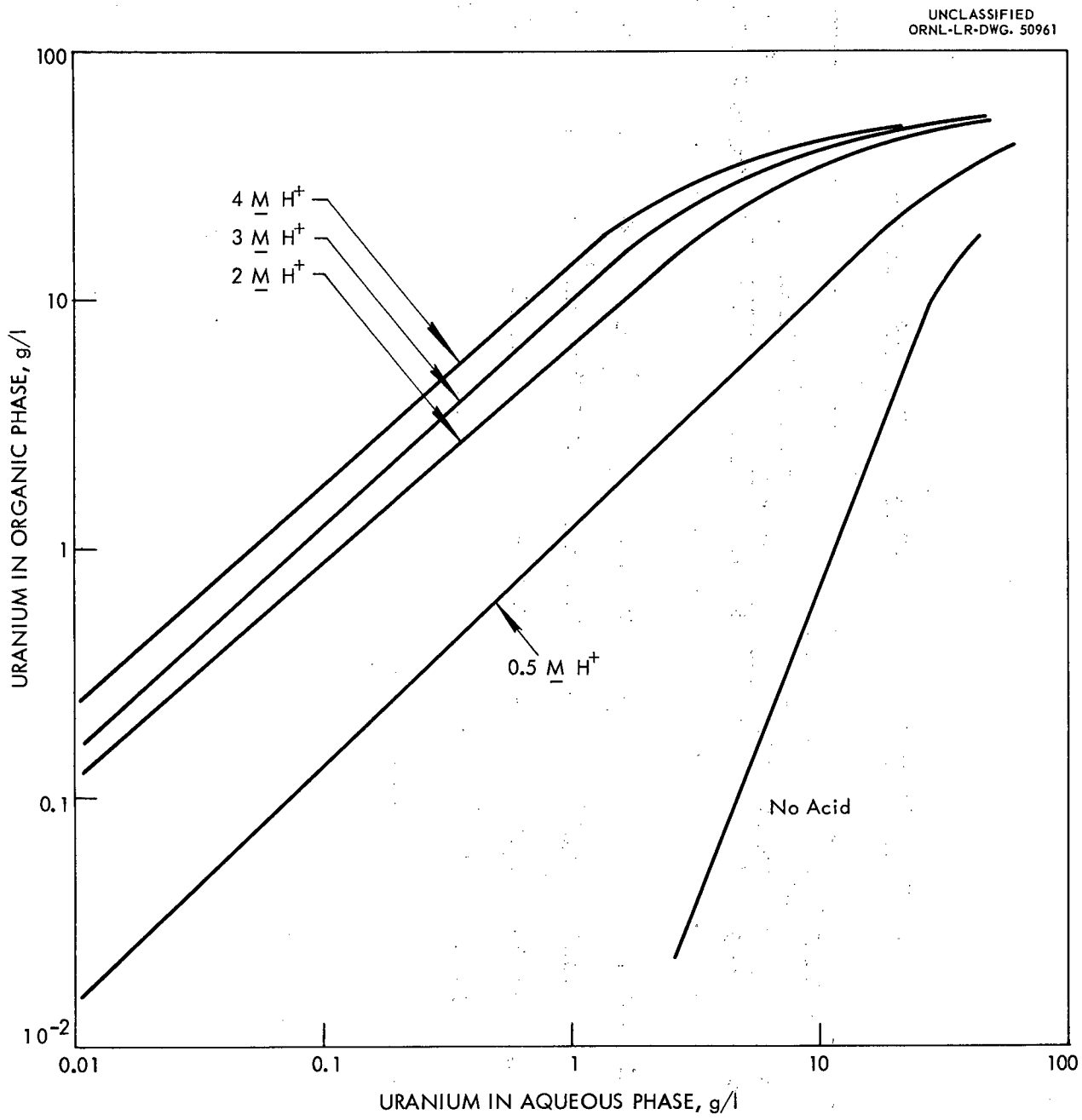

Fig. 17. Distribution of uranium between 15% TBP-Amsco and nitric acid solutions.

Table 4. Effect of TBP Concentration and Saturation on Decontamination

TBP Conc, %	At Feed Plate: Saturation U	Saturation H	Ext. Factor	Separation Factor Uranium/Contaminant: Gr γ	Ru γ	Zr-Nb γ	Th	Organic Product Decontamination Factor: Gr γ	Ru γ	Zr-Nb γ	Th	Ext. Stages	% U Equilibrium	% U Loss
2.8	38%	21%	2.25	9.7×10^{3}	$\geq5\times10^{3}$	200	15	2.7×10^{4}	$>2.7\times10^{3}$	>300	26	9	108	.001
5.26	68%	23%	-	6.3×10^{4}	1.3×10^{4}	700	22	2.6×10^{5}	2.3×10^{5}	4.3×10^{3}	25	7	76	.06
10.5	65%	27%	1.10	4.9×10^{4}	1.2×10^{4}	-	20	1.6×10^{5}	1.5×10^{4}	4.3×10^{3}	23	6	89	.02
15.0	61%	22%	1.11	3.0×10^{4}	6.7×10^{3}	≥350	26	1.3×10^{5}	3.5×10^{4}	$>3.1\times10^{3}$	38	5	92	.05

Table 5. Distribution of Uranium Between Nitric Acid Solutions and 5% TBP-Amsco

U_A	U_O	E_A^O	H_O	U_A	U_O	E_A^O	H_O
	No Acid in Feed				3.1 N HNO_3 in Feed		
0.980	0.001	-	-	0.019	0.090	4.74	0.10
2.92	0.004	0.0014	-	0.021	0.084	4.0	-
4.77	0.020	0.0042	-	0.062	0.228	3.68	-
9.80	0.120	0.012	-	0.134	0.384	2.87	-
19.4	0.522	0.027	-	0.214	0.769	3.59	-
27.0	1.34	0.050	-	0.244	0.830	3.40	0.10
35.4	2.49	0.070	-	1.28	3.62	2.83	-
45.0	4.00	0.089	-	1.39	3.76	2.71	0.08
51.4	5.14	0.10	-	3.45	7.13	2.07	0.07
	0.5 N HNO_3 in Feed			3.92	6.53	1.67	-
				9.58	10.50	1.10	-
0.087	0.017	0.195	~0.003	34.0	15.9	0.46	0.03
0.084	0.018	0.214	-	58.7	17.1	0.29	0.02
0.261	0.050	0.191	-	81.6	18.5	0.23	0.02
0.426	0.084	0.197	-				
0.842	0.163	0.194	-		4.1 N HNO_3 in Feed		
0.846	0.178	0.210	-	0.015	0.090	6.0	0.13
4.15	0.872	0.210	-	0.018	0.087	4.83	-
4.26	0.816	0.192	-	0.053	0.233	4.40	-
8.18	1.76	0.215	-	0.088	0.400	4.55	-
8.69	1.71	0.197	-	0.182	0.780	4.34	-
16.5	3.49	0.210	-	0.202	0.831	4.11	0.12
41.8	8.41	0.201	-	1.17	3.72	3.18	-
64.1	11.7	0.183	-	1.18	3.90	3.31	0.10
86.4	13.5	0.156	-	2.86	6.84	2.39	-
				3.01	7.00	2.33	0.09
	2.08 N HNO_3 in Feed			8.40	11.10	1.32	-
0.031	0.073	2.35	0.06	34.7	15.6	0.45	0.03
0.038	0.073	1.92	-	57.9	17.5	0.30	0.03
0.092	0.240	2.61	-	83.5	18.2	0.22	0.02
0.156	0.334	2.14	-				
0.316	0.665	2.10	-				
0.337	0.643	1.91	0.06				
1.85	3.10	1.68	0.05				
1.86	3.08	1.66	-				
4.29	5.78	1.35	-				
4.36	5.52	1.27	0.04				
10.1	9.01	0.89	-				
36.0	14.4	0.40	0.02				
59.2	14.4	0.28	0.02				
82.4	17.7	0.21	0.01				

Table 6. Distribution of Uranium Between Nitric Acid Solutions and 10% TBP-Amsco

U_A	U_O	E_A^O	H_O	U_A	U_O	E_A^O	H_O
	No Acid in Feed				3 N HNO_3 in Feed		
0.946	0.001	0.001	-	0.009	0.115	12.8	-
2.92	0.018	0.006	-	0.010	0.094	9.40	0.19
4.72	0.070	0.015	-	0.036	0.276	7.67	-
9.51	0.312	0.033	-	0.047	0.445	9.45	-
18.0	1.63	0.091	-	0.095	0.882	9.28	0.19
24.4	3.61	0.148	-	0.100	0.901	9.01	-
31.2	6.10	0.196	-	0.572	4.25	7.43	0.18
38.7	9.32	0.24	-	0.626	4.37	6.98	-
45.0	11.7	0.26	-	1.32	8.56	6.48	0.16
55.0	15.9	0.29	-	1.40	8.48	6.06	-
63.3	19.4	0.31	-	3.95	15.8	4.00	-
115	30.8	0.27	-	20.4	29.5	1.45	0.06
				40.9	33.1	0.81	0.04
	0.5 N HNO_3 in Feed			64.6	35.5	0.55	0.03
0.059	0.045	0.76	-		4 N HNO_3 in Feed		
0.061	0.041	0.70	0.01				
0.174	0.127	0.73	-	0.007	0.100	14.3	0.25
0.290	0.212	0.73	-	0.008	0.104	13.0	-
0.566	0.411	0.73	-	0.022	0.284	12.9	-
0.606	0.415	0.69	0.01	0.045	0.456	10.1	-
2.94	2.02	0.69	0.01	0.082	0.884	10.8	-
2.99	2.07	0.69	-	0.088	0.878	9.98	0.24
5.92	4.11	0.69	-	0.447	4.60	10.3	-
5.98	3.96	0.66	0.01	0.470	4.31	9.17	0.22
33.0	17.0	0.52	0.009	1.01	8.88	8.79	-
52.2	23.6	0.45	0.009	1.08	8.61	7.97	0.20
71.3	27.2	0.38	0.009	2.92	16.8	5.74	-
				19.4	29.5	1.52	0.08
	2.0 N HNO_3 in Feed			40.9	33.1	0.81	0.05
0.013	0.086	6.62	-	63.5	35.8	0.56	0.04
0.014	0.085	6.07	0.12				
0.043	0.265	6.16	-				
0.072	0.424	5.89	-				
0.147	0.854	5.81	-				
0.172	0.808	4.70	0.12				
0.833	3.93	4.54	0.11				
0.921	4.11	4.46	-				
1.84	8.08	4.39	-				
2.02	7.75	3.84	0.10				
5.16	14.9	2.89	-				
22.8	27.1	1.19	0.05				
43.1	31.0	0.72	0.04				
64.6	34.2	0.53	0.03				

Table 7. Distribution of Uranium Between Nitric Acid Solutions and 15% TBP-Amsco

U_A	U_O	E_A^O	U_A	U_O	E_A^O
No Acid in Feed			3 N HNO_3 in Feed		
0.996	0.0001	-	0.006	0.100	16.7
2.94	0.035	0.012	0.019	0.284	14.9
4.77	0.10	0.012	0.034	0.464	13.6
9.28	0.625	0.067	0.062	0.898	14.5
17.5	2.86	0.163	0.827	9.28	11.2
22.3	5.89	0.262	1.99	17.6	8.84
28.6	9.54	0.334	3.95	27.7	7.01
35.2	13.8	0.392	9.20	49.5	2.12
40.3	17.0	0.422	44.2	54.0	1.22
0.5 N HNO_3 in Feed			4 N HNO_3 in Feed		
0.045	0.064	1.42	0.005	0.120	24.0
0.135	0.188	1.39	0.014	0.300	21.4
0.230	0.320	1.39	0.024	0.520	21.7
0.451	0.610	1.35	0.052	0.916	17.6
2.25	2.85	1.27	0.265	4.66	17.6
4.51	5.56	1.23	0.625	9.01	14.4
9.14	10.49	1.15	1.41	18.7	13.3
15.3	16.5	1.08	3.21	29.0	9.03
24.0	24.2	1.01	7.90	40.8	5.16
38.3	32.9	0.86	22.1	50.0	2.26
56.8	40.8	0.70	44.2	54.7	1.24
2 N HNO_3 in Feed					
0.029	0.30	10.3			
0.050	0.48	9.60			
0.610	4.45	7.30			
1.22	8.80	7.21			
2.92	16.5	5.65			
5.79	26.3	4.54			
11.8	36.8	3.12			
26.3	46.0	1.75			
46.6	52.6	1.13			

Table 8. Effect of Irradiation of Feed on Acid Thorex Decontamination Factors

Flowsheet Conditions:

Feed: 275 g/l Th, 16 g/l U, 0.18 N AD, 1 volume, stage 1E

Scrub # 1: 0.01 M PO_4, 0.01 M $Fe(SO_3NH_2)_2$, 0.8 volume, stage 6E

Scrub # 2: 5.0 M HNO_3, 0.2 volume, stage 3S

Acid: 13 M HNO_3, 0.5 volume, stage 4E

Solvent: 30% TBP-Amsco, 7 volumes, stages 5E

Stages: 5 extraction, 6 scrub

Irradiation, w/hr/l	Decontamination Factor				Th Loss	Th Balance	Feed Age (Days)
	Gross γ	Ru γ	Zr-Nb γ	Pa γ			
			Series # 1				
Control	2,500	370	3,300	≥1,200	0.11%	105%	2
5.1	1,900	1,200	1,900	≥1,100	0.10%	107%	1
10.3	1,500	350	1,400	~1,800	0.07%	105%	6
41	6,530	970	7,000	~2,800	0.10%	107%	7
41	5,700	1,300	4,640	2,400	0.05%	104%	9
165	16,000	1,800	18,000	>2,100	0.07%	106%	20
			Series # 2				
165	31,000	1,400	>310	-	0.46%	106%	3
Control	5,800	356	150	-	0.45%	101%	4
167	14,000	2,000	>290	-	0.41%	100%	10
Control	2,400	470	130	-	0.43%	100%	11

Table 9. Distribution of Uranium, Thorium and Nitric Acid Between 30% TBP-Amsco and Solutions Containing 100 to 200 g/l Thorium and 0 to 0.2 N Nitric Acid

U_A	U_O	E_A^O	Th_A	Th_O	E_A^O	H_O
		100 g/l Th - No Acid in Feed				
0.013	0.082	6.3	73.4	24.9	0.34	
0.041	0.224	5.5	71.0	23.8	0.34	
0.064	0.400	6.3	71.6	24.6	0.34	
0.118	0.760	6.4	68.7	24.5	0.36	
0.648	4.36	6.7	71.6	23.9	0.33	
1.39	8.73	6.3	74.6	23.4	0.31	
2.96	17.2	5.8	76.0	20.1	0.26	
4.60	24.7	5.4	77.5	18.7	0.24	
6.61	33.1	5.0	80.4	17.4	0.22	
		150 g/l Th - No Acid in Feed				
0.013	0.076	5.9	103	42.7	0.41	
0.032	0.248	7.8	105	42.2	0.40	
0.057	0.450	7.9	108	43.9	0.41	
0.105	0.890	8.5	104	42.7	0.41	
0.555	4.26	7.7	108	43.8	0.41	
1.16	8.93	7.7	110	40.2	0.37	
2.43	16.80	6.9	113	37.0	0.33	
3.86	25.80	6.9	118	34.7	0.29[a]	
5.56	33.1	6.0	120	40.7[a]	0.34[a]	
		200 g/l Th - No Acid in Feed				
0.010	0.080	8.0	140	56.1	0.40	
0.030	0.240	8.0	142	53.4	0.38	
0.059	0.410	6.9	142	53.7	0.38	
0.119	0.966	8.1	142	52.9	0.37	
0.554	4.17	7.5	142	51.6	0.36	
1.11	8.18	7.4	142	50.6	0.36	
2.32	17.1	7.4	145	46.5	0.32	
3.69	25.6	6.9	152	43.2	0.28	
5.14	34.3	6.7	156	38.0	0.24	
		200 g/l Th - 0.2 N H in Feed				
0.009	0.078	8.7	103	43.3	0.42	0.04
0.03	0.205	6.8	103	42.1	0.41	0.04
0.059	0.405	6.9	103	41.2	0.40	0.04
0.113	0.966	8.5	103	43.0	0.42	0.04
0.567	4.35	7.7	105	41.2	0.40	0.04
1.21	8.70	7.2	107	36.3	0.34	0.03
2.51	17.1	6.8	111	36.8	0.33	0.04
4.09	26.1	6.9	111	33.3	0.30	0.06
5.54	36.3	6.6	116	31.0	0.28	0.05

[a] Probably analytical error.

The controls and each of the irradiated feeds were heated to 55°C with 0.2 M $NaHSO_3$ for 1 hr prior to solvent extraction.

In this series a single control run was compared to the group of runs using irradiated feeds and therefore, the possibility existed that the improvement in decontamination factor was due to the aging of the feed solution. In the second series of experiments using a newly prepared feed solution, controls were run the day following each irradiation run. Again however the experiments using highly irradiated feeds (165 watt-hr/liter) resulted in gross γ decontamination factors more than 5 times greater than with the control.

Duplicate experiments using feed aged an additional week showed decontamination lower by a factor of 2 for both the irradiated feed and the control.

1.2.3 Distribution Coefficients

Distribution coefficients are being determined for the extraction of uranium in various alternative processes which are being proposed for the processing of Consolidated Edison fuel. High reflux of thorium in a long partitioning column results in thorium concentrations up to 40 g/liter in the organic phase.[16] The data published in a previous report[17] has therefore been extended to include uranium distribution when the organic phase contains 15 to 60 g/l thorium or ~40 g/liter thorium-0.05 N HNO_3 (Table 9, Fig. 18). These data demonstrate the very small variation in uranium distribution coefficients in this range. Due to the coextraction of the thorium, the distribution coefficients of the uranium in this system are about the same as the distribution coefficients in 1 N HNO_3 systems.

The extraction of uranium by 2.5% TBP-Amsco from solutions containing 30 g/liter thorium with no acid and with 2 N HNO_3 has been determined in order to evaluate the possibility of an Interim-23 type second thorium cycle flowsheet without an intercycle evaporator (Table 10, Fig. 19). In this range of conditions, the uranium distribution may be closely predicted using the total nitrate values previously published[18] for uranium extraction with 2.5% TBP-Amsco from nitric acid solutions.

Table 10. Distribution of Uranium Between 2.5% TBP-Amsco and Solutions Containing 28 g/l Thorium or 29 g/l Thorium and 2.1 M Nitric Acid

U_A	U_O	E_A^O	U_A	U_O	E_A^O
28 g/l Th - No Acid in Feed			29 g/l Th-2.1 N HNO_3 in Feed		
0.097	0.006	0.062	0.067	0.040	0.60
0.279	0.006	0.022	0.158	0.158	1.00
0.474	0.009	0.019	0.270	0.250	0.93
0.911	0.021	0.023	0.546	0.521	0.95
4.74	0.166	0.035	3.02	2.10	0.70
9.61	0.434	0.045	6.63	3.34	0.50
18.4	0.863	0.047	14.64	5.17	0.35

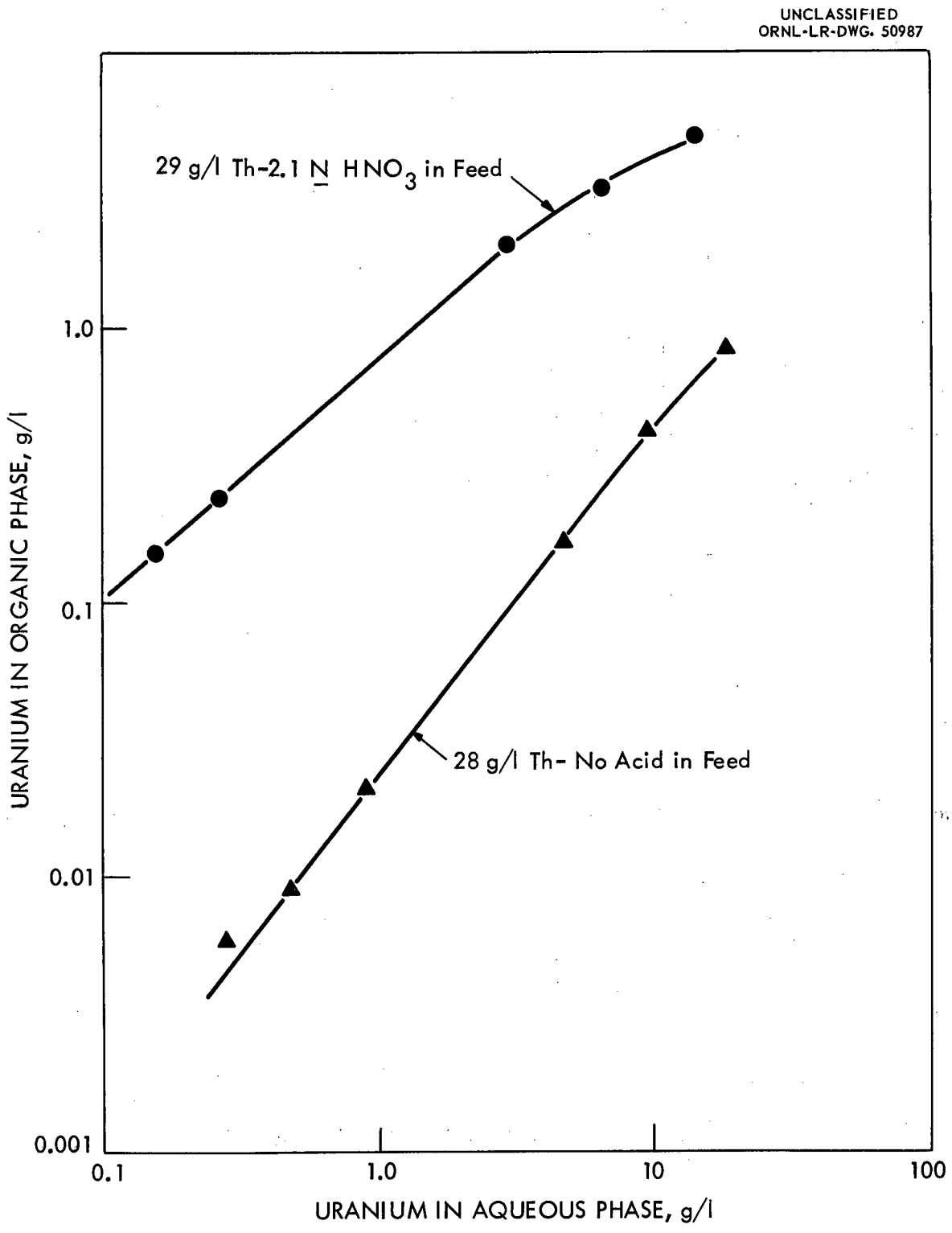

Fig. 18. Distribution of uranium between 2.5% TBP-Amsco and solutions containing 28 g/l thorium or 29 g/l thorium-2.1 N HNO_3.

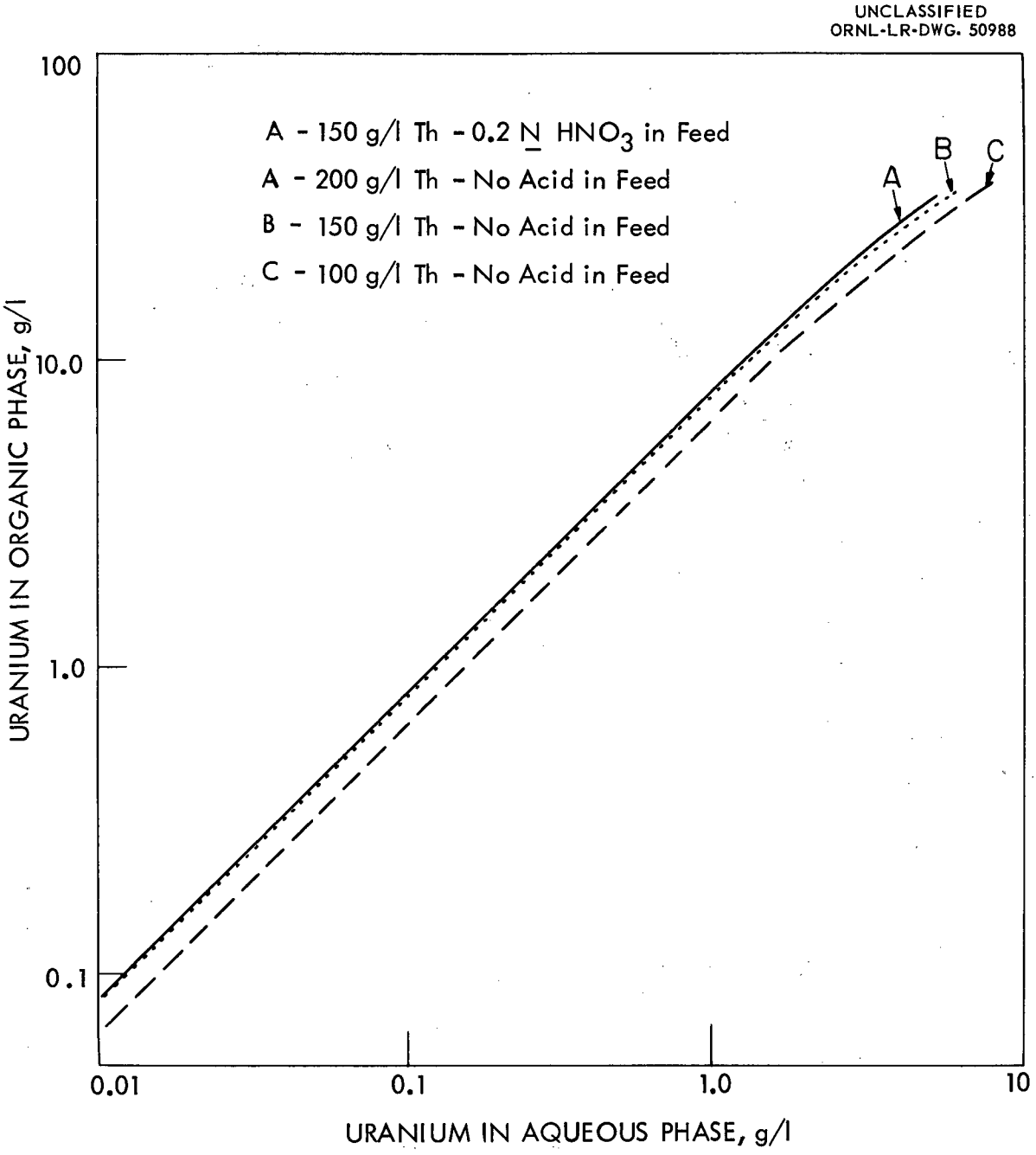

Fig. 19. Distribution of uranium between 30% TBP-Amsco and solutions containing 100 to 200 g/l thorium.

1.3 Corrosion Studies (Work done by members of the Reactor Experimental Engineering Division) (W. E. Clark)

During the month of June 1960, corrosion studies have continued on titanium during Thorex feed-adjustment boildowns, on Ni-o-nel in Thorex solutions, on two Haynes experimental alloys in Sulfex solutions and on stainless steel and Ni-o-nel in simulated Darex-Purex waste solutions. In addition, scouting tests were run to evaluate the corrosion rate of titanium in the HNO_3-Fe(III) and nitric acid, fluoroboric acid, and ammonium dichromate solutions proposed for dissolution of U-Mo core alloys.

1.3.1 Thorex Process

Exposure of titanium in and above refluxing Thorex feed adjustment solutions has been continued to a total of 1902 hr for the bottoms. In addition exposure of titanium specimens in and above refluxing initial feed adjustment solution is being repeated using a solution 0.3 M borate instead of 0.1 M as previously reported.[19] After 168 hr exposure in the condenser above the initial solution, titanium showed an over-all rate of 3.74 mils/mo whereas tantalum showed a small weight gain (Table 11). In the condenser above the refluxing bottoms the maximum over-all rate of titanium was 0.48 mil/mo. As has been consistently observed in previous tests, the attack on the condenser specimen was localized primarily in the weld and heat-affected zones. Metallographic examination of the titanium cover for the dissolver employed in former tests in this system indicates that the two welds most severely attacked were made with Ti-A-110-AT (~5% Al, 2.5% Sn, balance Ti-45A) filler rod rather than with Ti-55AX rod as was desired.

After 48 batch boildowns (~175 hr) of the boron-containing FAT solution, negligible corrosion has been observed on the titanium-45A weld specimens and the titanium dissolver cover used in these boildowns.

A special low-carbon Ni-o-nel from stock obtained for construction of the Sulfex-Thorex dissolver and having the chemical composition shown in Table 12 has been tested in beginning Thorex solutions containing boron, aluminum, and thorium in various concentrations. Butt-welded specimens were fabricated from 1/4-in.-thick plate in the as-received condition using filler rod prepared from the parent material. The corrosion rates observed over 96 hr exposure varied from a maximum of 11.5 mils/mo in solution containing 0.05 M $Na_2B_4O_7$ as the only additive to 2.6 mils/mo in solution containing 0.1 M $Al(NO_3)_3$ and 0.1 M $Th(NO_3)_4$ as well as 0.05 M $Na_2B_4O_7$ (Table 13). In every case the over-all rates for the solution specimens were less than corresponding rates for the best specimen previously tested[19] (heat-treated to 1800°F before welding) while the rates for the vapor-phase specimens were about the same in both cases. More significant is the fact that the specimens of low-carbon Ni-o-nel appeared to be essentially free of localized attack in the heat-affected zone of the weld. This means that the low-carbon Ni-o-nel is more superior to the other specimen than is indicated by comparative rates since the real criterion is maximum penetration rather than general attack.

Table 11. Corrosion Rates of Welded Titanium-45A and Tantalum Specimens in Thorex Feed Adjustment Tests

A. Total Reflux of Initial FAT Solution.[a]

Specimen Position	Corrosion Rate (mpm) 168 hr	
	Ti-45A	Ta
C[b]	3.74	g
V	0.24	g
I	g	g
S	g	g

B. Total Reflux of Bottoms[c] from Boildown Tests.

	1680 hr	1902 hr
C[b]	0.42, 0.44	0.44, 0.48
V	0.01, 0.04	0.03, g
I	g , g	g , g
S	g , g	g , g

[a] 9.5 M HNO_3, 0.04 M NaF, 0.04 M $Al(NO_3)_3$, 0.07 M $UO_2(NO_3)_2$, 0.8 M $Th(NO_3)_4$, 0.3 M H_3BO_3, 0.002 M HCl, 0.004 M $Fe(NO_3)_3$.

[b] Condenser specimens.

[c] 1.0 M HNO_3, 0.15 M NaF, 0.13 M $Al(NO_3)_3$, ~0.20 M $UO_2(NO_3)_2$, 2.6 M $Th(NO_3)_4$, 0.64 M H_3BO_3, 0.006 M HCl, 0.013 M $Fe(NO_3)_3$.

Table 12. Chemical Composition of a Special Low-Carbon Ni-o-nel Prepared by Vacuum-Induction Melting

Element	Weight Per Cent
Carbon	0.005
Sulfur	0.002
Manganese	0.09
Silicon	0.22
Chromium	21.25
Nickel	41.91
Molybdenum	3.10
Titanium	0.17
Aluminum	0.08
Copper	2.23
Iron	Balance

Table 13. Corrosion of Low-Carbon Ni-o-nel[a] in Various Thorex Solutions

Solution Comp.[b]	Corrosion Rate (mpm)											
	24 hr			48 hr			72 hr			96 hr		
	V	I	S	V	I	S	V	I	S	V	I	S
1	12.9	9.5	9.3	12.0	8.4	7.8	12.0	8.1	7.3	11.5	8.0	7.0
2	4.2	3.2	2.8	3.6	3.5	2.3	3.4	2.3	2.1	3.2	2.1	1.9
3	11.5	7.5	7.2	10.4	6.3	6.0	10.2	6.2	5.6	10.0	6.0	5.3
4	3.6	2.5	2.4	3.0	2.0	2.0	2.8	1.9	1.8	2.6	1.7	1.6

[a] Fabrication history unknown.

[b] 1. 13.0 M HNO_3-0.04 M NaF-0.05 M $Na_2B_4O_7$.
2. 13.0 M HNO_3-0.04 M NaF-0.05 M $Na_2B_4O_7$-0.1 M $Al(NO_3)_3$.
3. 13.0 M HNO_3-0.04 M NaF-0.05 M $Na_2B_4O_7$-0.1 M $Th(NO_3)_3$.
4. 13.0 M HNO_3-0.04 M NaF-0.05 M $Na_2B_4O_7$-0.1 M $Al(NO_3)_3$-0.1 M $Th(NO_3)_3$.

1.3.2 Titanium in HNO_3-HBF_4-$(NH_4)_2Cr_2O_7$ Solutions

Specimens of titanium-45A were tested in various solutions capable of dissolving zirconium, with and without dissolving Zircaloy-2 present. These solutions consisted of 3.0 to 15.0 M HNO_3, 0.5 M HBF_4, and 0.3 M $(NH_4)_2Cr_2O_7$ (Table 12). The actively dissolving Zircaloy-2 lowered the observed attack rate by a factor greater than two in most, though not all of these tests. Maximum solution phase rates varied from 19 mils/mo in 3 M HNO_3 in the presence of dissolving zirconium to 295 mils/mo in 9 M HNO_3 in the absence of zirconium (Table 14). Although the corrosion rates are much lower than might be expected in solutions containing such high concentrations of fluoride they are still too high to allow consideration of titanium as a container material for dissolution of zirconium fuels in such solutions.

Table 14. Corrosion Rates of Titanium-45A in Boiling Fluoride-Containing Solutions[a]

(24-hr test)

HNO_3 Solution (M)	Corrosion Rate (mpm)					
	No Zirconium Present			Presence of Dissolving Zirconium		
	V	I	S	V	I	S
3.0	3.1	40.0	50.0	0.5	16.0	19.0
9.0	19,16	110,120	150,150	1.6,1.1	66,130	140,140
12.0	4.7,35	170,175	260,295	2.9,2.0	110,29	110,110
15.0	1.0,1.9	180,210	270,270	1.7,1.7	94,77	180,190

[a] All solutions contain 0.5 M HBF_4-0.3 M $(NH_4)_2Cr_2O_7$.

1.3.3 Sulfex Process

Additional tests conducted on Haynes experimental alloys, EB4358 and EB5459 in Sulfex solutions confirmed the suspicion that the cause of the localized attack observed at the weld edges of both alloys[19] was associated with strains resulting from the shearing process. The edge of each specimen used in these tests was polished on a belt sander until approximately 0.025 in. of material had been removed. After 144 hr in test, the surfaces of both alloys were uniformly attacked, with some random pitting observed. There was no visible preferential attack on the weld edges of either alloy. Although the rates observed (Table 15) are about a factor of 3 greater than those reported last month,[19] this reflects the effect of a dilute nitric acid rinse which was used to remove a copper-colored deposit found on the solution and interface specimens after each 24-hr test period.

Table 15. Corrosion of Alloys EB4358 and EB5459 in Boiling Sulfuric Acid with Dissolved Stainless Steel[a]

Specimen Position	Alloy	Corrosion Rate (mpm)					
		24 hr	48 hr	72 hr	96 hr	120 hr	144 hr
V	EB4358	0.74	1.01	0.99	0.98	0.97	1.05
	EB5459	1.28	1.36	1.50	1.40	1.43	1.49
I	EB4358	1.09	2.28	1.81	1.94	1.70	1.75
	EB5459	1.41	2.40	1.94	2.07	1.80	1.81
S	EB4358	1.14	2.31	1.71	1.71	1.54	1.67
	EB5459	0.87	2.14	1.63	1.65	1.46	1.53

[a]Solution consisted of 10 g/liter of Type 304L stainless steel dissolved in fresh 6.0 M H_2SO_4 solution.

1.3.4 Waste Storage Tests

A scouting test at 80°C using specimens of Ni-o-nel in high-acid simulated waste solution was terminated after 431 hr because of severe intergranular attack suffered by the solution specimen. No additional tests using Ni-o-nel are planned.

The weight loss observed on both 304L and 347 stainless steels continues to follow the trend indicated in the data plotted and reported last month[19] at both 50 and 65°C. The tests will, therefore, be terminated after about 2200 hr, and selected specimens from these and all previous waste storage tests will be submitted for a metallographic examination in order to confirm the type and extent of attack suffered by the 304L and 347 stainless steels in these tests. Tests are planned which should give some insight as to the cause for the intergranular attack observed on specimens in the solution and interface phases of these solutions.

1.3.5 Molybdenum Core Alloy Solutions

Tests have been initiated to investigate the corrosion behavior of titanium-45A in solutions expected to be encountered during the aqueous dissolution of molybdenum core alloys. The dissolvent planned for these fuels is 3-8 M HNO_3 with 0.5 M $Fe(NO_3)_3$ added to complex the molybdenum. In tests designed to compare the corrosion of solutions containing varying concentrations of nitric acid both with and without dissolution products over-all rates were found to be low ($\leq$0.24 mil/mo) in all cases (Table 16). The beginning solution, 3 M in HNO_3 gave the lowest corrosion rate throughout the test period of 72 hr, but the data are so erratic that no further correlation appears to be justified at the present time. Examination of the specimens by low-power optical microscope indicated that some localized attack in the form of irregular, shallow depressions had occurred. The tests will, therefore, be continued until the type and extent of attack can be determined. Additional tests are planned in these same solutions using specimens of a special low-carbon Ni-o-nel.

Table 16. Corrosion of Titanium-45A in Various Molybdenum Core Alloy Solutions

HNO_3 Concentration (M)	Corrosion Rate (mpm)								
	24 hr			48 hr			72 hr		
	V	I	S	V	I	S	V	I	S
3.0[a]	g	0.02	0.02	0.01	0	0	0.04	0.03	0.01
3.0[b]	0.24	0.17	0.21	0.05	0.02	g	-	-	-
5.0[a]	0.11	g	0.12	0.03	0.02	0.05	0.04	0.02	0.04
5.0[b]	0.04	0	0	-	-	-	-	-	-
8.0[a]	0.13	0.15	0.02	0.05	0.10	0.02	0.24	0.10	0.03
8.0[b]	0.09	g	0	-	-	-	-	-	-

[a]Solutions contained 0.5 M $Fe(NO_3)_3$.

[b]Solutions contained 0.5 M $Fe(NO_3)_3$-0.6 M $UO_2(NO_3)_2$-0.02 M MoO_3.

1.4 Mechanism of Separation Methods (W. Davis, Jr.)

1.4.1 Radiation Damage to Solvents and Diluents (Work performed at Stanford Research Institute under Subcontract 1081)

Of particular interest in studies of the radiolysis of TBP are yields of formation of the acid degradation products dibutyl phosphoric acid (HDBP), monobutyl phosphoric acid (H_2MBP), and orthophosphoric acid (H_3PO_4). If the TBP-diluent solutions are anhydrous or contain only water as a third component, then the quantities of HDBP and H_2MBP formed by radiation decomposition of TBP can be determined by electrometric titration. When nitric acid is also dissolved in the TBP-diluent solution, analyses for the acidic degradation products becomes very difficult. Recent work has been largely devoted to developing analytical procedures to overcome this difficulty. A procedure[20] that appears very promising for determining HDBP, H_2MBP, and H_3PO_4 in TBP-Amsco 125-82 solutions that also contain water and nitric acid is as follows: 1) use ascending paper chromatography to separate the acids; 2) cut the paper strips into ~0.5 cm lengths; 3) irradiate the paper sections in a neutron field of $\sim 10^{13}$ $n/cm^2 \cdot sec$ for 1 hr; 4) determine the P-32 on each piece after a cooling time of about 2 weeks. This cooling period is required to permit decay of Na^{24} formed by reaction of sodium in the paper by the reaction Na^{23} (n,γ) Na^{24}. Although results from various tests have already suggested certain modifications in techniques, data from two samples of TBP-Amsco-HNO_3 diluted with known quantities of HDBP, H_2MBP, and H_3PO_4 have already shown a sensitivity down to 0.2 micrograms of phosphorus and accuracies in the order of ± 20%, Table 17.

Table 17. Phosphorus Analysis by Paper Chromatography and Neutron Activation Techniques

	Phosphorus in Sample, micrograms	
	By Analysis	As Prepared
Sample 1[a]		
TBP	24.8	30.4
HDBP	1.30	1.15
H_2MBP	1.48	1.87
H_3PO_4	0.383	0.274
Sample 2[b]		
TBP	24.8	29.3
HDBP	6.18	5.81
H_2MBP	1.54	1.88
H_3PO_4	1.58	1.40

[a] One microliter of 1 M TBP-Amsco-1 M HNO_3 spiked with ~1% HDBP, 1% H_2MBP, and 0.1% H_3PO_4.

[b] One microliter of 1 M TBP-Amsco-1 M HNO_3 spiked with ~5% HDBP, 1% H_2MBP, 0.5% H_3PO_4.

1.4.2 Solubility of Ferric Mono- and Dibutyl-Phosphates in Process Solutions (W. Davis, Jr.)

Mono- and dibutyl phosphoric acids, which are products of the thermal or radiolytic decomposition of TBP, react with iron(III) to form solids that have on occasion caused difficulties in operating solvent extraction plants. In order to obtain quantitative information on factors influencing the precipitation of these iron(III) butyl phosphates, each was prepared as a nearly pure solid and then used in studies of its solubility in aqueous and TBP-Amsco solutions. Five solutions of 30% TBP in Amsco 125-82 were contacted with equal volumes of aqueous solutions containing 0 to 3.9 M HNO_3. The two phases were separated and placed in graduated cylinders after which solid iron(III) monobutyl phosphate or iron(III) dibutyl phosphate was added to each in quantities sufficient to exceed solubilities. Each solution was agitated for approximately 4 weeks and sampled after 2 and 4 weeks in order to determine if saturation had been achieved.

Solubilities of ferric dibutyl phosphate were below the spectrographic limit of detectability, $\sim 10^{-5}$ M, in all organic solutions tested, wherein the nitric acid concentration varied from 0 to 0.71 M. In the aqueous phases, the solubility increased from less than 1×10^{-5} M in water to $\sim 4 \times 10^{-4}$ M in 3.2 M HNO_3 (Fig. 20). Solubilities of ferric monobutyl phosphate in the acidic aqueous and TBP-Amsco solutions increased from 1.8×10^{-4} to 8×10^{-2} and $< 1.4 \times 10^{-4}$ to 3.4×10^{-2} M, respectively, as the nitric acid concentration in the aqueous phase increased from 0 to 2.96 M and that in the organic phase from 0 to 0.64 M (Fig. 20). These data show that ferric dibutyl phosphate precipitation will occur in a solvent extraction system when the concentrations of Fe(III) and HDBP are both as low as ~10-50 ppm providing the aqueous phase acidity is below ~0.1 M HNO_3.

2.0 WASTE TREATMENT
(J. T. Roberts)

2.1 Evaporation and Calcination of Purex Waste (H. W. Godbee, F. R. Clayton)

A synthetic Purex 1WW waste (Table 18) containing magnesium and additional sodium was semi-continuously evaporated and calcined to 900°C. The experimental

Table 18. Composition of Simulated Purex 1WW Concentrate

(Molarity)

H^+	NO_3^-	$SO_4^=$	Na^+	Fe^{+3}	Al^{+3}	Cr^{+3}	Ni^{+2}	Ru
5.6	6.1	1.0	0.6	0.5	0.1	0.01	0.01	0.002

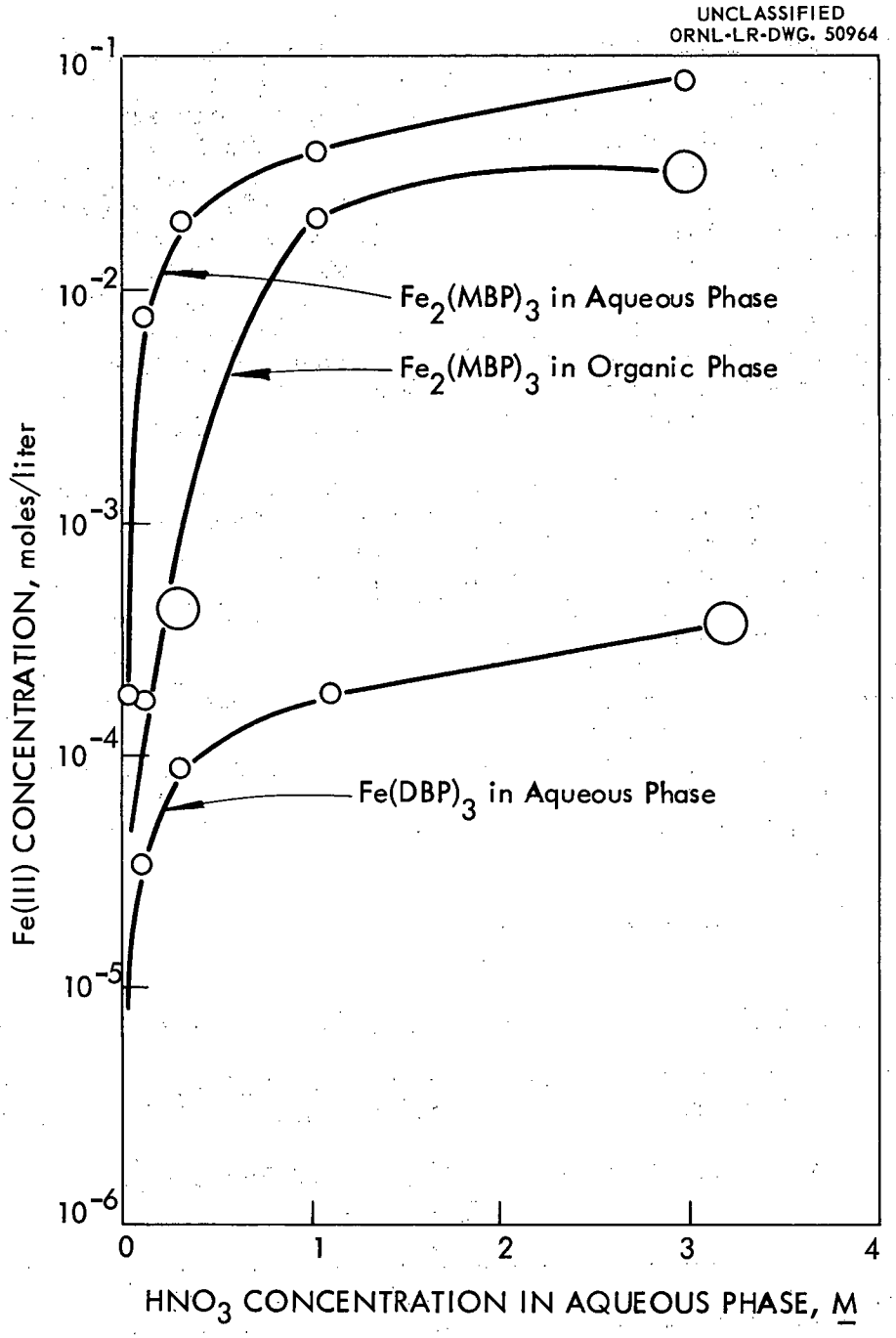

Fig. 20. Solubility of ferric monobutyl phosphate in aqueous and 30% TBP-Amsco-HNO_3 solutions and of ferric dibutyl phosphate in aqueous HNO_3 solutions.

apparatus (Fig. 21) consisted of a feed system, a 4 in. o.d. x 18 in. long stainless steel calciner pot in a 5 kw furnace, and an off-gas handling system. The feed rate, adjusted to equal the boil-off rate of the pot, declined throughout the experiment from 100 ml/min initially to almost nothing at the end of the evaporation period. Nitric oxide (NO) was added to the system (a closed system) during the experiment to prevent any build-up of free oxygen from nitrate destruction. The addition of NO to the system was regulated so that the pressure in the system was atmospheric or slightly sub-atmospheric.

Sodium was added as 50% NaOH solution (1.2 moles NaOH per liter of 1WW) and magnesium as MgO (0.2 mole /liter of 1WW). The criteria for addition of these materials were that the equivalents of sodium plus magnesium be greater than the equivalents of sulfate, to prevent sulfate volatility, and that the equivalents of sulfate be greater than the equivalents of sodium, to prevent sodium-cesium volatility.

A volume reduction factor, volumes of Purex 1WW fed/volume of solid residue, equal to 7 was obtained. The solid residue had an apparent density, weight of solid/bulk volume of solid, equal to 1.32 g/ml, which is equivalent to a porosity of 58%. The condensate, residue, and scrub liquid contained 87, 12, and 1.4%, respectively, of the initial weight of waste fed. The condensate and off-gas scrub liquid contained 91 and 9%, respectively, of the feed nitrate. Of the original sulfate, 0.28% was in the condensate and 0.02% in the off-gas scrub liquid. Since the residue has not been removed from its can, pending additional thermal conductivity measurements, nitrate and sulfate analyses of the residue are not available. Analyses for stable ruthenium showed that 32% of the original feed ruthenium was in the condensate and none in the scrub liquid.

The fraction of the ruthenium found in the condensate above is about 20 times higher than in earlier small scale batch experiments with the same Purex-Na-Mg mixture. Perhaps the mode of operation, i.e., batch as opposed to semi-continuous, accounts for part of this difference. In other words, the concentrations, especially of acid, in the calciner vessel for the quasi-steady state conditions of semi-continuous operation are possibly different at all times from those in the pot of a simple batch operation. Possibly another reason for the high ruthenium concentration in the condensate is the fact that the stainless steel vessel and lines used in the present experiment had been used in a previous evaporation and calcination of a similar waste. Consequently, some of the ruthenium in the condensate could be ruthenium which had plated out in the earlier experiment and washed off by nitric acid into the condensate of the present experiment.

The production of off-gas, previously shown to be essentially oxygen for evaporation and calcination without nitric oxide,[21] was essentially zero in this experiment with nitric oxide added.

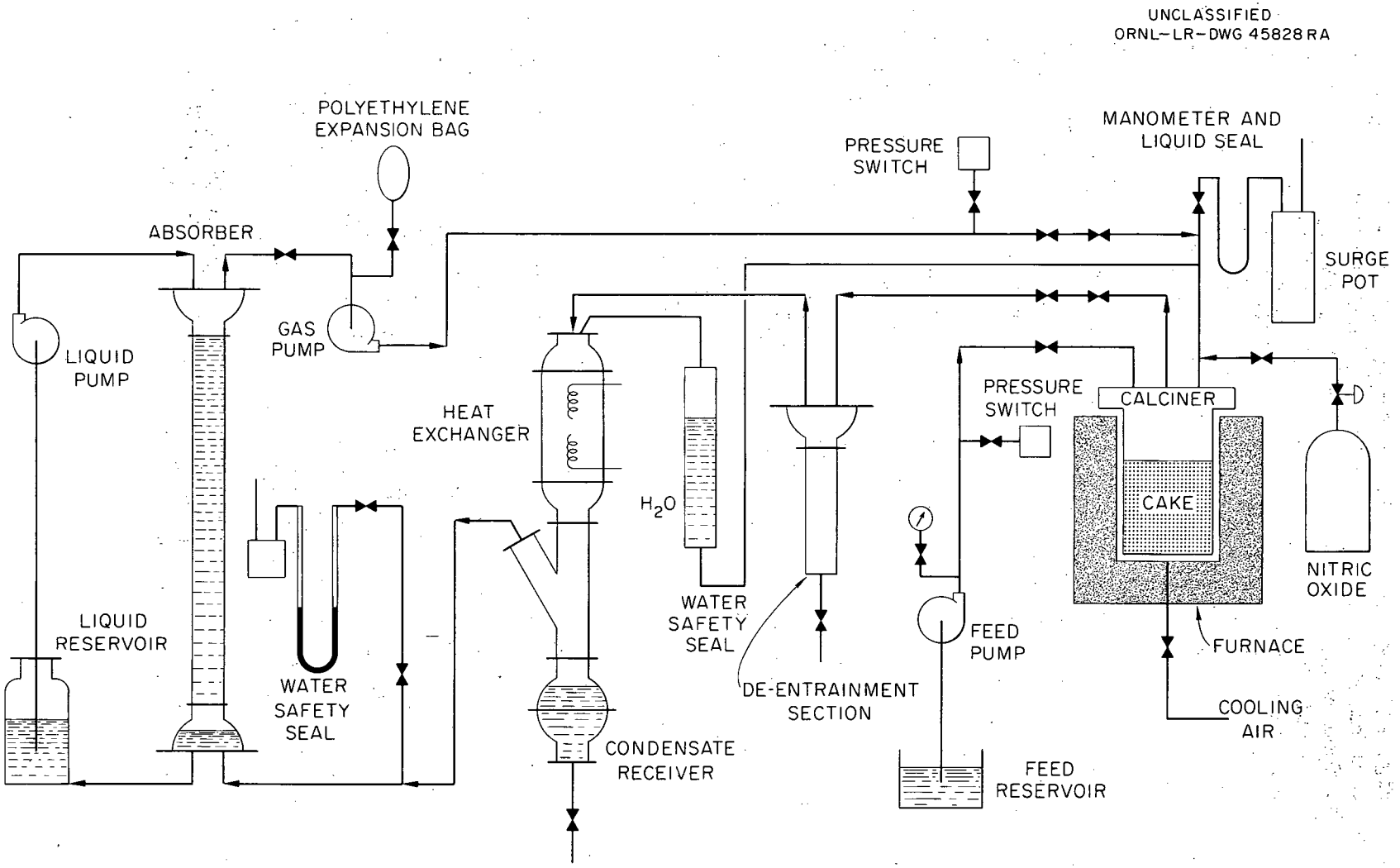

Fig. 21. Schematic of apparatus for calcining wastes and scrubbing volatile ruthenium from off-gas.

2.2 Thermal Conductivity of Calcined Wastes (H. W. Godbee, W. C. Ripka)

Thermal conductivity, k, has been determined experimentally for the calcined Purex 1WW waste (Table 18) plus magnesium (0.2 moles/liter of 1WW) and additional sodium (1.2 moles/liter of 1WW) described above. The measurements indicate that k is 0.155 Btu/hr-ft-°F at 475°F and 0.207 Btu/hr-ft-°F at 676°F. The thermal conductivity was determined by a steady state method employing radial heat flow in a hollow cylinder.[22] The cylinder had an i.d. of 1/2-in., an o.d. of 4 in., and was 18 in. long.

These values of k are slightly less than those reported previously[21] for a calcined Purex 1WW (Table 18) plus calcium (0.2 moles/liter of 1WW) and additional sodium (1.2 moles/liter of 1WW). The previous residue, porosity of 48%, gave values for k of 0.236 and 0.254 Btu/hr-ft-°F (smoothed data) at the temperatures mentioned above.

2.3 Volatility of Ruthenium during Waste Evaporation and Calcination (H. W. Godbee, F. R. Clayton, W. C. Ripka)

Experiments were performed to study the effect of various additives and a nitric oxide (NO) atmosphere on ruthenium volatility when simulated Purex 1WW waste (Table 18) is evaporated and calcined. The various additives (Table 19) were included for the purpose of reducing sulfate volatility from Purex when it is calcined. Nitric oxide was swept through the evaporator to maintain a reducing atmosphere in order to suppress ruthenium volatility. Samples of Purex 1WW containing 0.184 g/l of stable ruthenium and 0.1 $\mu c/ml$ of Ru-106 tracer plus additives were evaporated and calcined to about 500°C. The experimental apparatus consisted of a glass flask, a glass condenser, a heating mantle, and stainless steel sheathed thermocouples for recording temperatures in the liquid-solid and vapor phases.

Purex 1WW containing no additives with nitric oxide sweep gas gave 1.5% of the feed ruthenium in the condensate (Table 19 and Fig. 22). Sodium and calcium additives increased the per cent of the ruthenium in the condensate to 17-32%. Substituting magnesium for calcium (mole for mole) gave 2-15% ruthenium in the condensate, depending upon the amount of sodium (Table 19 and Fig. 22).

2.4 Thermochemical Studies of Waste Components (W. E. Tomlin)

Thermogravimetric analysis was made of $NaHSO_4 \cdot H_2O$. The curve (Fig. 23) shows a plateau at 50% weight loss at 700°C to 950°C. This corresponds to the formation of Na_2SO_4 which was verified by x-ray analysis.

2.5 Treatment of Decladding Wastes for Disposal (W. E. Tomlin)

Results show that briquettes made with Portland cement, sand and water, cured for three weeks and then, heated to 300°C for 24 hr have less compression strength than those made with calcium aluminate cement. Unheated briquettes made with Portland cement had much less compression strength than those made with calcium aluminate cement.

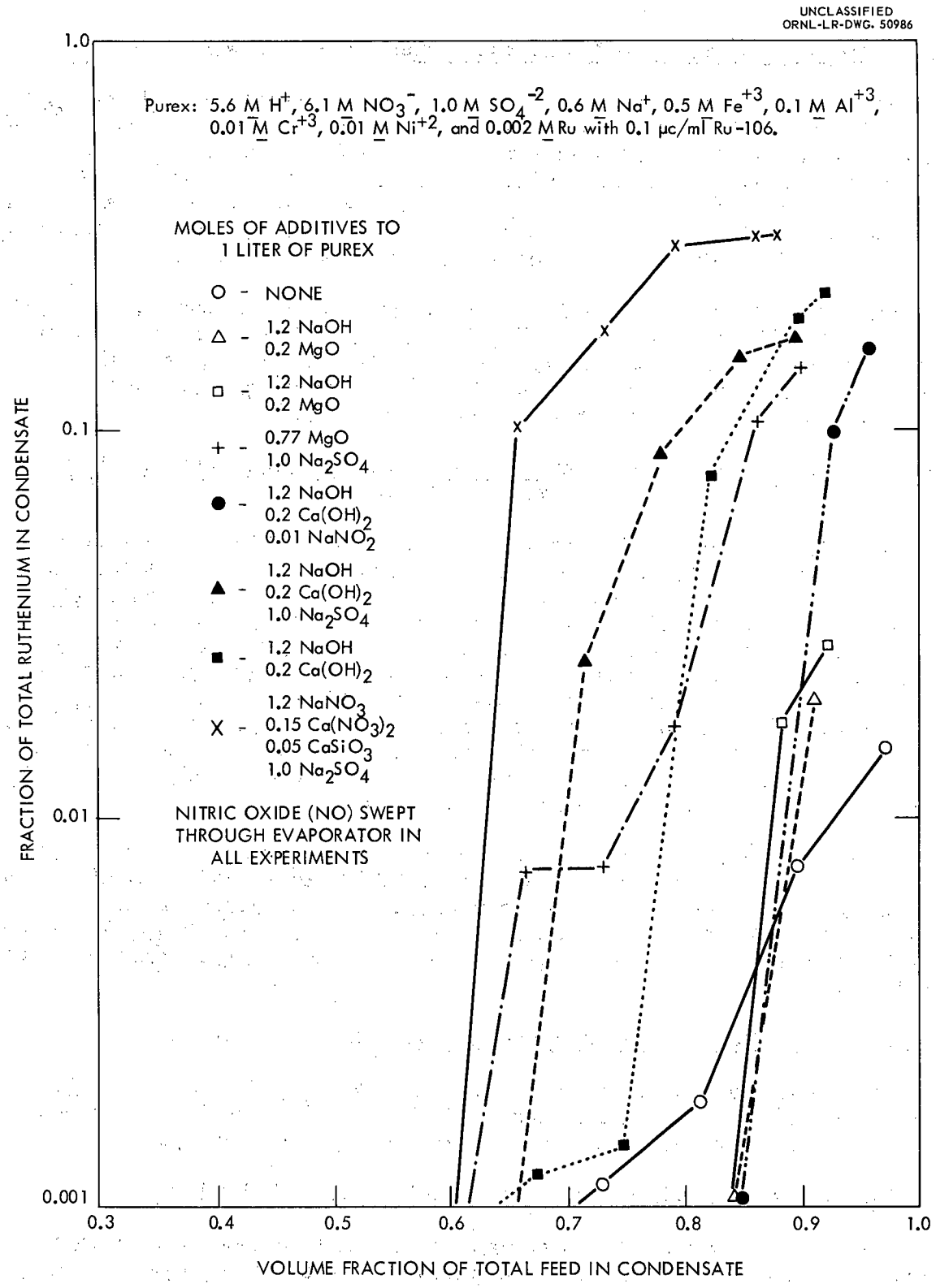

Fig. 22. Volatility of ruthenium during evaporation of Purex 1WW concentrate in glass equipment.

Table 19. Batch Evaporation of Purex 1WW in Glass Equipment

Composition of Purex 1WW: 5.6 M H^+, 6.1 M NO_3^-, 1.0 M SO_4^{-2}, 0.6 M Na^+, 0.5 M Fe^{+3}, 0.1 M Al^{+3}, 0.01 M Cr^{+3}, Ni^{+2}, and 0.002 M Ru

Exp.	Additives to 1 liter of Purex 1WW (moles)	Sweep Gas	Final Temps. of Residue, °C	Approx. Vol of Residue (ml)	Visible Ru Deposit on Equipment	Max. Ru Conc. in Condensate (Fraction of Feed Conc.)	Total Ru in Condensate (% of that in feed)
1	None	Nitric Oxide (NO)	485	63	No	0.10	1.5
2	NaOH.....1.2 MgO 0.2	Nitric Oxide (NO)	490	36	No	0.27	2.0
3	NaOH .....1.2 MgO 0.2	Nitric Oxide (NO)	490	45	No	0.26	2.8
4	MgO .....0.77 Na_2SO_4 .....1.0	Nitric Oxide (NO)	480	48	Yes	1.15	14.9
5	NaOH .....1.2 $Ca(OH)_2$ .....0.2 $NaNO_2$ 0.01	Nitric Oxide (NO)	530	42	Yes	2.54	17.4
6	NaOH .....1.2 $Ca(OH)_2$ .....0.2 Na_2SO_4 .....1.0	Nitric Oxide (NO)	535	62	Yes	1.10	17.4
7	NaOH .....1.2 $Ca(OH)_2$ 0.2	Nitric Oxide (NO)	545	31	Yes	2.13	22.9
8	$NaNO_3$ .....1.2 $Ca(NO_3)_2$ ....0.15 $CaSiO_3$ .....0.05[a] Na_2SO_4 .....1.0	Nitric Oxide (NO)	480	61	No	1.82	32.6

[a]Added as Micro-Cel E, a Johns Manville synthetic calcium silicate.

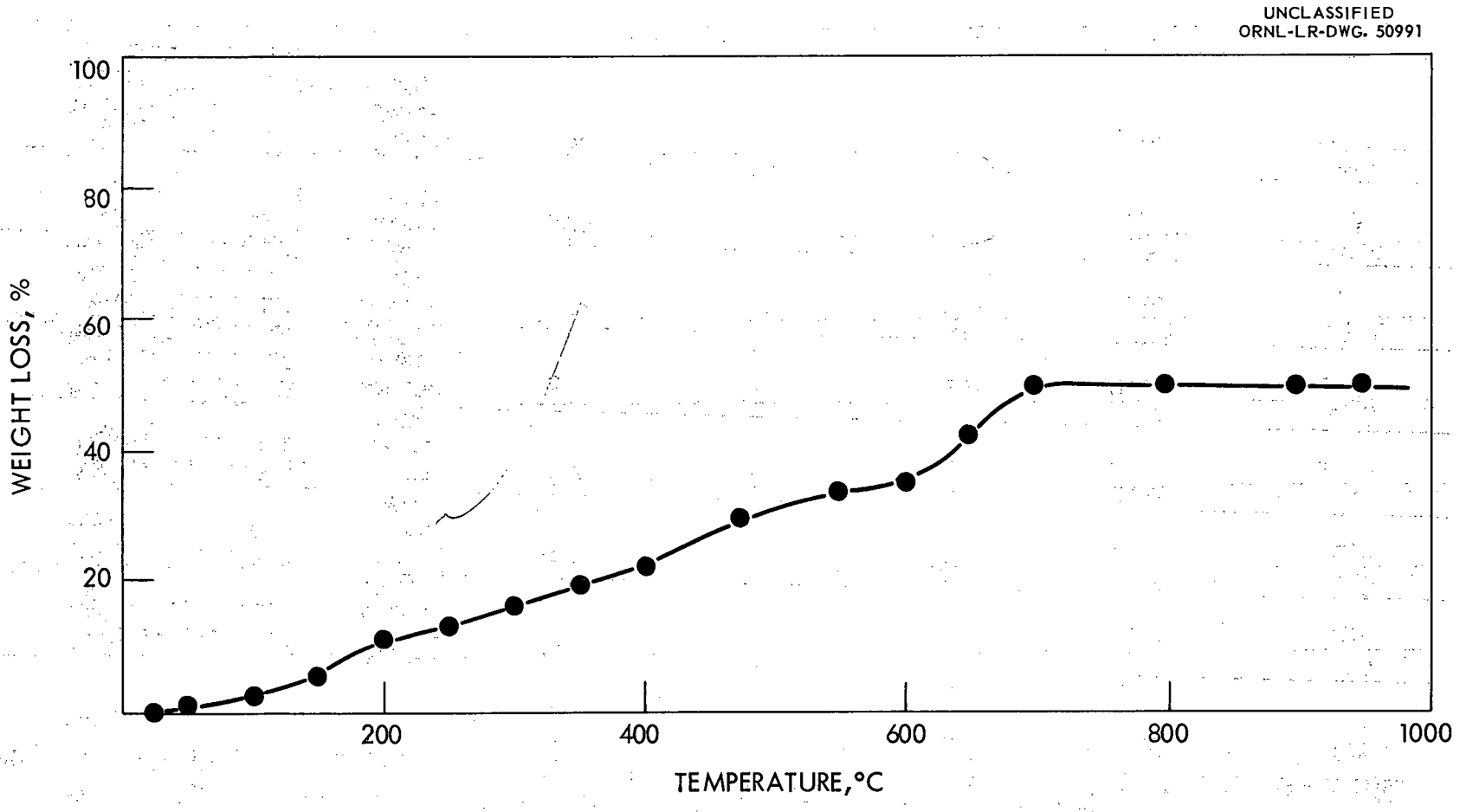

Fig. 23. Thermogravimetric analysis of $NaHSO_4 \cdot H_2O$.

Briquettes having the following composition (parts by weight): water 1.0, Portland cement 1.86, Ottawa sand 6.81 were cured for 3 weeks at room temperature then heated to 300°C for 24 hr. Other briquettes having the same composition but made with a heat resistant cement (calcium aluminate) were tested under the same conditions. The results are given in Table 20.

Table 20. Cement Composition - Temperature - Compression Test

2-in. cube briquettes

Temperature, °C	Portland Cement Compression Test, psi	Calcium Aluminate Cement Compression Test, psi
Unheated 25°	5,700	14,400
Heated 300°	4,600	5,800

2.6 Low Level Waste Treatment by Ion-Exchange (R. R. Holcomb)

Laboratory development work was continued to evaluate ion exchange processes as methods for treating low level process wastes.

The effect of Versene (EDTA), which may be present in low level wastes, on the efficiency of the proposed ion-exchange process was determined in two experiments. In the first, the waste contained 0.64 g disodium Versenate (10 ppm as EDTA). The second was a duplicate except that it did not contain Versene (Fig. 24). The synthetic waste solutions were made up using tap water and Cs, Ce, and Sr radioisotope tracers. After adjustment to 0.01 M NaOH and filtration, the solutions were passed through identical 19.2 ml Na^+ form Duolite C-3 columns (1/2 in. i.d. x 6"). The effluent activity from the Versene run started out somewhat higher than that from the control run, however, they reached the same level just before the breakthrough (0.1% level) occurred for both runs at slightly over 1500 bed volumes of waste. About 99.9% (d.f. = 1000) of the gross gamma activity was removed by the combined precipitation, filtration and ion-exchange steps.

The Duolite CS-100, carboxylic phenolic cation exchanger, which compared favorably with Duolite C-3 in loading characteristics, has been eluted (Fig. 25) upflow with 2.5 M HCl regenerant solution at a rate of 37.5 ml/hr. The highest effluent activity reading of 8.6×10^7 cpm/ml was reduced by a factor of 10^3 in 3.4 bed volumes of 2.5 M HCl, a considerable improvement over the 7.6 bed volumes of 5 M HCl required to reduce the effluent activity of Duolite C-3 by the same factor. Shrinkage of the Duolite CS-100 to 2/3 of its original volume when contacted with the acid eluant is the main disadvantage. This disadvantage in plant operation would necessitate an upflow rinse under fluidized bed conditions with sufficient NaOH to convert the entire bed to the Na^+ form prior to the next loading cycle.

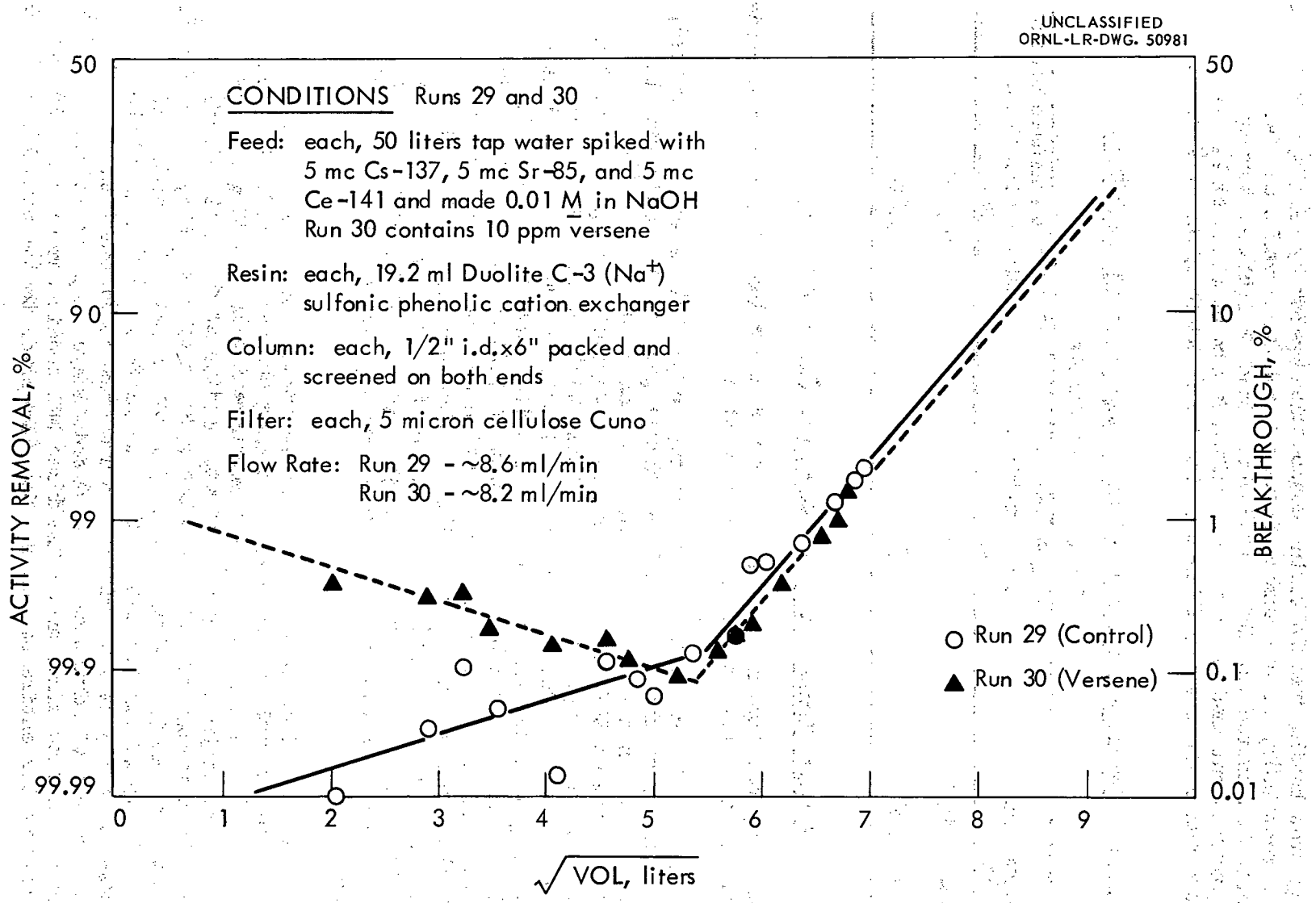

Fig. 24. Three-day loading cycle - synthetic process waste water on Duolite C-3.

An activity reduction of 10^3 was demonstrated on Duolite CS-100 resin with 7 bed volumes of 1 M HCl regenerant in an upflow elution (Fig. 25) at 37.5 ml/hr. While less acid is required with the 1 M eluant than with the 2.5 M eluant (3.4 bed volumes), the time required for complete regeneration may make the higher concentration regenerant more attractive for elution of CS-100 resin.

A 19.2 ml Duolite C-3, sulfonic phenolic cation exchanger, resin column which had been exhausted with approximately 1500 bed volumes of simulated process water waste, was eluted upflow with 4.0 M HCl at a rate of 40 ml/hr (Fig. 26). The effluent activity was reduced by a factor of 10^3 with 10 bed volumes of the 4.0 M HCl regenerant. This compares marginally with the 10^3 activity reduction factor obtained with 8 bed volumes of 5.0 M HCl regenerant in a similar experiment (Fig. 26). The elution characteristics of this resin are poorer than the CS-100. However, as shown previously the acid value of the effluent can be reclaimed and recycled by evaporation, thus the amount of acid consumed in the regeneration cycle may not be the most important factor in selecting the resin to be used.

In order to determine the efficiency of previously loaded and eluted resins in a second cycle demonstration, two runs (Fig. 27) were made, one with Duolite C-3-sulfonic phenolic exchanger and one with Duolite CS-100-carboxylic phenolic exchanger. For this study, 7.9 mc Cs^{137}, 7.8 mc Sr^{85}, and 7.8 mc Ce^{141}, were added to 100 liters of actual process water waste, made 0.01 M in NaOH, filtered on a 5 micron cellulose Cuno filter and divided into two separate 50 liter containers. These two feed solutions were passed simultaneously through two identical columns (1/2 in. i.d. x 6 in.) at a flow rate of 6.25 ml/min each. Cerium, amounting to approximately 0.5% of the total activity in the filtered feed, appeared in the effluent from both columns almost immediately. A cesium activity breakthrough occurred on the CS-100 column after 1518 bed volumes of waste were treated. The run was terminated after 2133 bed volumes without the appearance of strontium in the effluent. The effluent from the C-3 column remained constant at the 0.5% breakthrough level, resulting from cerium, for 1938 bed volumes of waste. Gamma energy scans indicated the start of Cs-Sr breakthrough at this point. The over-all gross gamma decontamination resulting from precipitation, filtration and ion-exchange amounted to 99.7% (d.f. = 340) activity removal from 1518 bed volumes of wastes with Duolite CS-100 and 1938 bed volumes with Duolite C-3.

In order to measure the effectiveness of Duolite C-3 for removing strontium from process water waste, 50 liters of actual waste spiked with 5 mc Sr^{85} and made 0.01 M in NaOH was passed through 19.2 ml of this resin. The results (Fig. 28, Run 36) were similar to previous runs, showing no significant Sr breakthrough after a throughput of 2100 bed volumes of waste. Simultaneously with the above run, unspiked process waste which was also made 0.01 M in NaOH was passed through an identical column. The effluent samples from the Sr spiked run contained more than twice the activity of the samples from the unspiked run, yet no Sr^{85} could be detected in either, possibly indicating an impurity in the Sr^{85} tracer isotope.

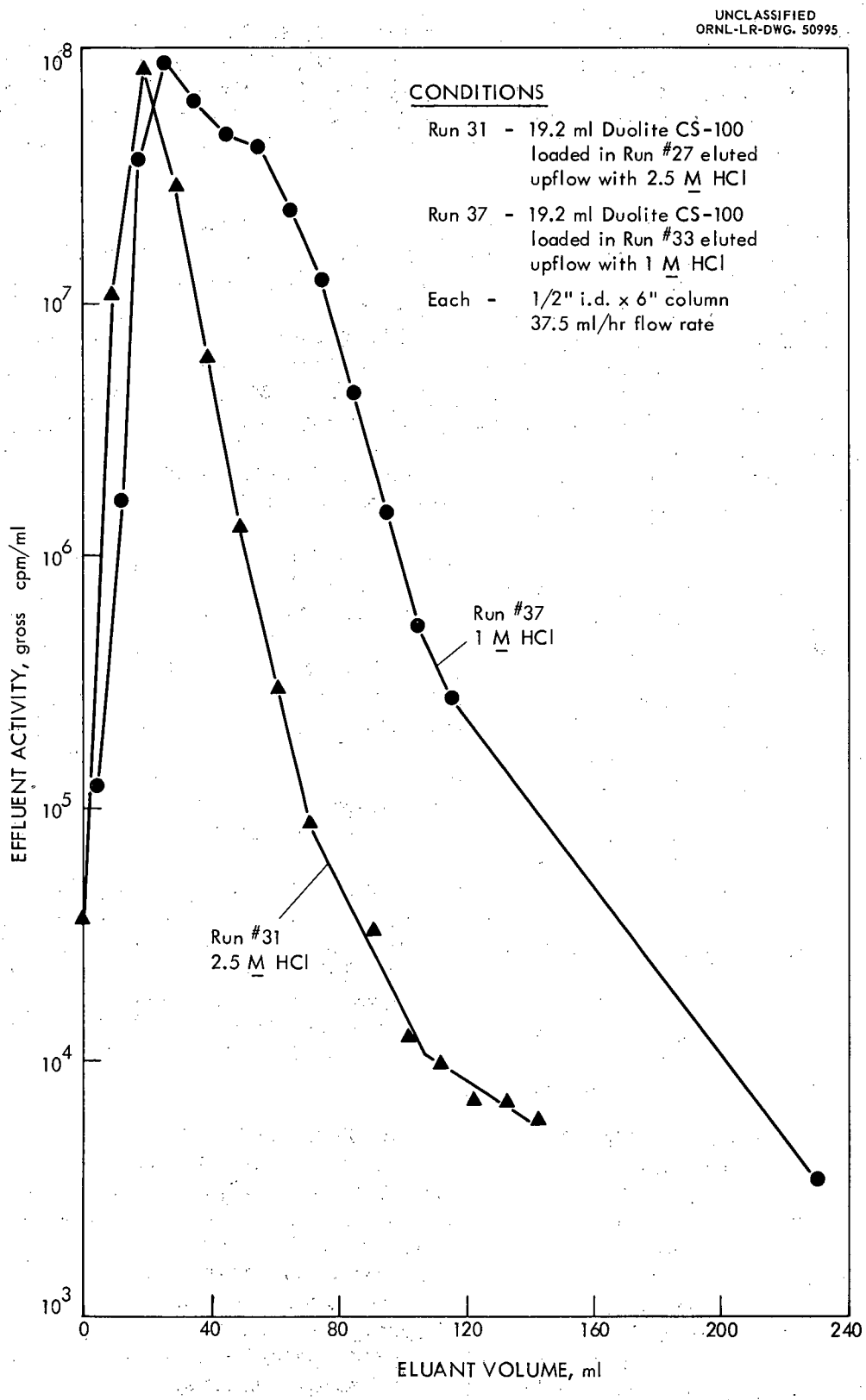

Fig. 25. Upflow elution of Duolite CS-100.

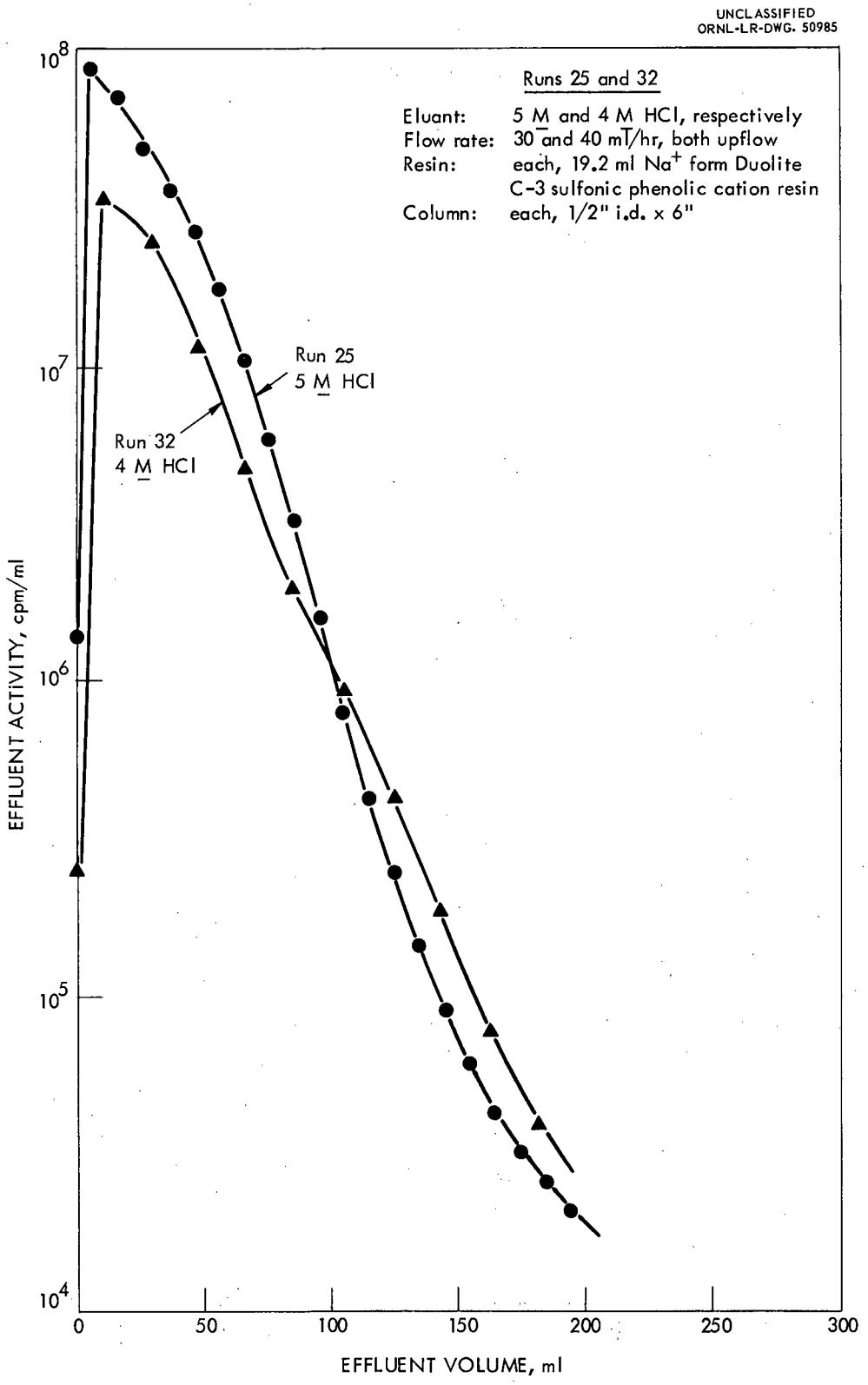

Fig. 26. Upflow elution of activity from Duolite C-3.

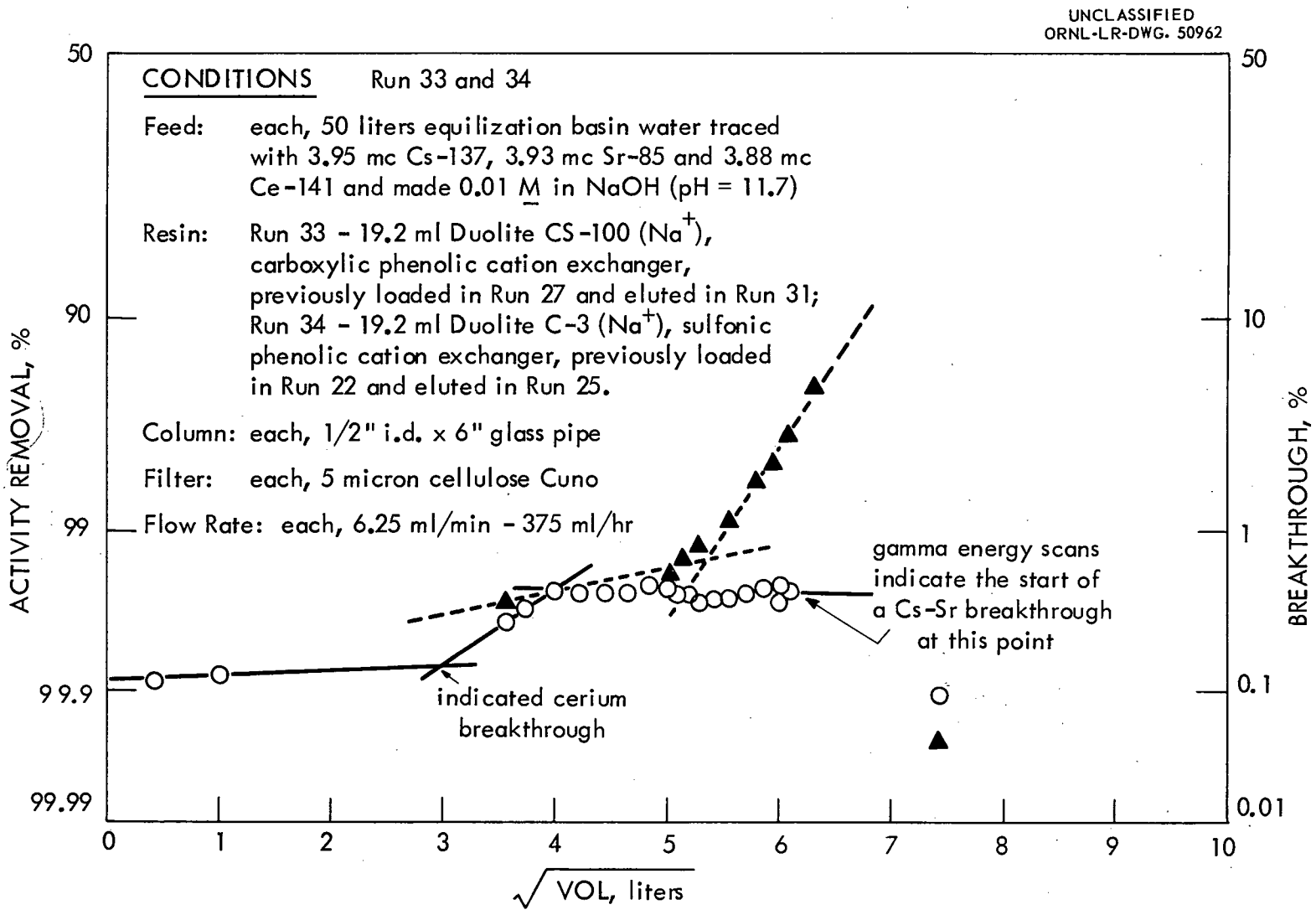

Fig. 27. Second cycle loading curves for Duolite C-3 and Duolite CS100.

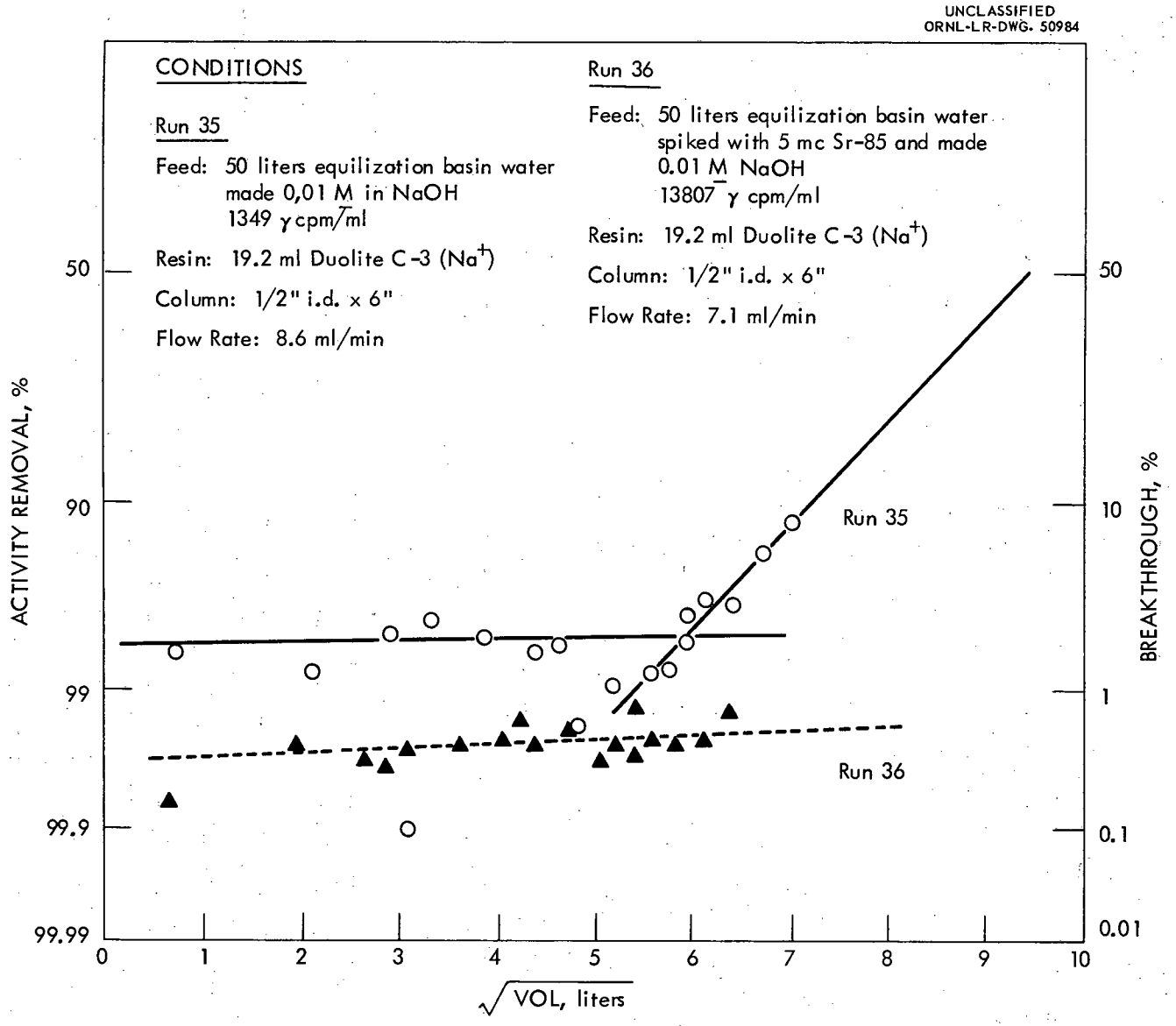

Fig. 28. Loading of Duolite C-3 with untreated and Sr-85 spiked actual waste.

Two runs have been completed to demonstrate the primary reason for selecting phenolic base resins in preference to styrene base resins (Fig. 29). One hundred liters of actual process water waste was spiked with 9 mc Sr^{85}, 10 mc Cs^{137}, and 10 mc Ce^{141}, made 0.01 M in NaOH and filtered on a 5 micron Cuno filter. Half of this feed solution was passed (8.8 ml/min) through 19.2 ml of Na^+ form Duolite C-20, styrene base sulfonic acid cation exchanger. A 70% activity breakthrough, representing approximately 100% of the cesium in the feed, occurred early in the run. However, no Sr^{85} could be detected in the effluent from the column, even after the passage of 2300 bed volumes of waste. Simultaneously, the second 50 liters of feed was passed (7.1 ml/min) through 19.2 ml Na^+ form Duolite CS-100 (3rd cycle). Cesium broke through (1% level) after 1500 bed volumes of waste, which is comparable with the previous two cycles on this resin column. This resin also effectively removed Sr from the 2300 bed volumes of waste treated.

3.0 ION EXCHANGE
(J. T. Roberts)

3.1 Fission Product Recovery by Ion Exchange (W. C. Yee)

The individual fission product concentrations in the synthetic Purex waste concentrate had to be increased to simulate the composition of the waste solution from low burn-up reactors. The basis for this study was the design specifications for the Yankee Atomic Reactor.[23] Estimated quantities of each fission product were calculated with the aid of the data of Blomeke and Todd.[24] However, correction factors for thermal neutron flux and irradiation time had to be applied to this data in order to correspond to Yankee Reactor nuclear conditions. These corrected fission product concentrations were then reduced by a factor of 10 to approximate low burn-up reactor conditions. Table 21 lists the corrected individual fission product concentrations for Yankee Reactor conditions. Table 22 gives the corrected concentrations of the compounds added to the waste solution which would be representative of the radiochemicals present for a low burn-up reactor. The concentration of major chemical constituents and the respective compounds used in making a synthetic waste solution remained unchanged and is reported in Table 23.

The capacity of Dowex 50W X-8 (20-50 mesh) resin for rare earths was determined using as feed 10X diluted supernatant from the adjusted synthetic Purex waste concentrate, made 0.124 M in oxalic acid. Approximately 0.1 mc/liter each of Ce^{144}-Pr^{144}, $Eu^{152-154}$, and Y^{91} were included in the feed as tracer material. A flow rate of about 20 ml/min was maintained through a column containing 40 ml of resin. This was equivalent to a flow rate of almost 3X that of previous runs using 150 ml of resin (27 ml/min). The 50% breakthrough for rare earths occurred at about 74 resin volumes.

Small amounts of iron sorbed on the resin column were removed by passing about 10 resin volumes of 1 M HNO_3-0.124 M oxalic acid through the resin column at 20 ml/min.

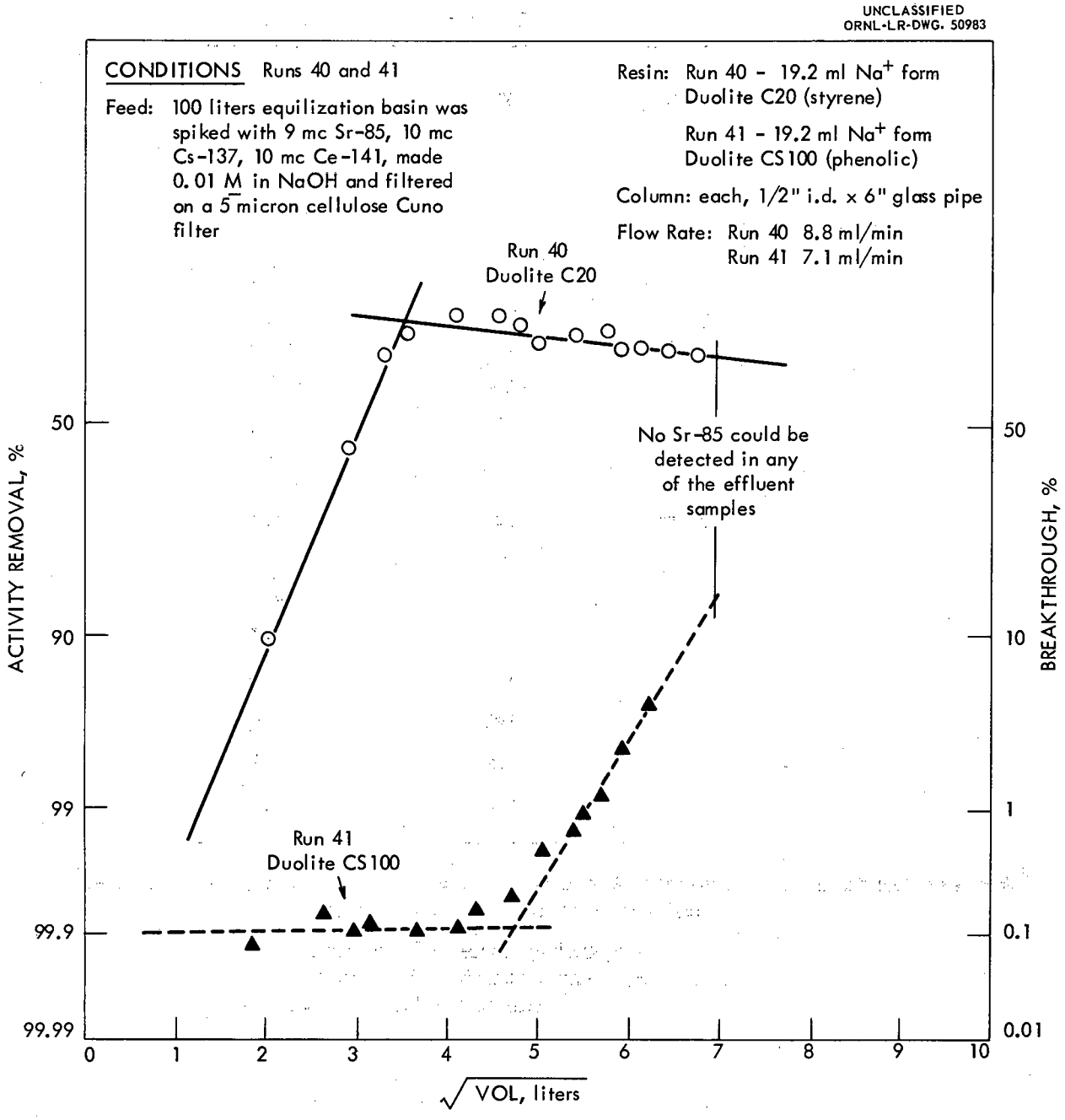

Fig. 29. Loading of actual (spiked) waste on phenolic and styrene base cation resins.

Table 21. Amount of Fission Products in Purex Waste Solution Under Yankee Atomic Reactor Conditions[a]

	Fission Product	g/mt U
Light	Rb	113
	Sr	289
	Y	146
	Zr	974
	Nb	14
	Mo	782
	Tc	204
	Ru	388
	Rh	98
	Pd	50
Heavy	Cs	671
	Ba	274
	La	281
	Ce	728
	Pr	274
	Nd	935
	Pm	104
	Sm	134

[a]Nuclear Conditions: Average thermal flux = 1×10^{13} neutrons/$cm^2 \cdot sec^{-1}$
Irradiation time = 417 days
cooling time = 100 days
Initial U-235 enrichment = 3.4 atom %
Burnup = 7600 Mwd/mt U

Table 22. Fission Products in Purex Waste Concentrate for Low Burnup Reactor (10% of Yankee)

	Conc. (g/l)	Chemical Used	Formula Weight	Amount Chemical per Liter Waste Solution
Pb	0.073	$RbNO_3$	148	0.126 g
Sr	.185	$Sr(OH)_2 \cdot 8H_2O$	266	0.562 g
Zr	.624	$ZrO(NO_3)_2$	1 M soln, 81 g Zr/l	7.7 ml
Nb	.009	Nb(metal)	92.9	0.009 g
Mo	.501	Mo(metal)	95.9	0.501 g
Ru	.249	$RuNO(OH)_3 \cdot H_2O$	200	0.492 g
Rh	.063	$Rh(NO_3)_3$	10% soln, sp. G = 1.05	1.69 ml
Pd	.032	$Pd(NO_3)_2$	231	0.069 g
Cs	.430	$CsNO_3$	195	0.631 g
Ba	.176	$Ba(OH)_2 \cdot 8H_2O$	316	0.405 g
La	.180			
Ce	.467			
Pr	.176	Re_2O_3 Mixture	309 (avg)	3.614 g
Nd	.600	Lindsay Mixture[a]	1110	
Sm	.086			
Y	.094			

[a]Rare earth mixture produced by Lindsay Chemical Company, West Chicago, Ill.

La	20-25%	Nd	15-20%
Ce	25-30%	Sm	7-10%
Pr	7-10%	Y	6-12.5%

Table 23. Make-up of Synthetic Purex Waste Concentrate

	Conc., M	Chemical Used	Molecular Weight	Amount Chemical per Liter Waste Solution
H^+	5.6	-	-	-
NO_3^-	6.1	HNO_3	63	268 ml of 15.9 M
$SO_4^=$	1.0	H_2SO_4	98	38.7 ml of 18.1 M
Na^+	0.6	$Na_2SO_4 \cdot 10H_2O$	322	96.6 g
Al^{+++}	0.1	$Al(NO_3)_3 \cdot 9H_2O$	375	37.5 g
Fe^{+++}	0.5	$Fe(NO_3)_3 \cdot 9H_2O$	404	202 g
Cr^{+++}	0.01	$Cr(NO_3)_3 \cdot 9H_2O$	400	4.00 g
Ni^{+++}	0.01	$Ni(NO_3)_2 \cdot 6H_2O$	291	2.91 g
UO_2^{++}	0.01	UO_3	286	2.86 g
$PO_4^=$	0.01	30% TBP in Amsco	-	2.7 ml TBP in 6.3 ml Amsco
$SiO_2 \cdot xH_2O$	0.02	H_2SiO_3	78	1.56 g

The rare earths were eluted by pumping 0.5 M mono-sodium citrate (pH 3.5) upwards through the loaded resin column at the slow flow rate of 0.5 ml/min. The elution was slow; after approximately 25 resin volumes of eluant had passed through the resin, the activity of the effluent had decreased gradually by 500-fold. Apparently, slow kinetics is responsible. After allowing the resin column to soak for about 1-1/2 days in citrate solution, the eluant was pumped through slowly again. The activity level of the effluent went as high as 1.4×10^4 cpm/ml before slowly returning to its initial 0.05×10^4 cpm/ml (Fig. 30). The efficiency of the citrate elution would probably be greater at higher temperatures.

3.2 Radiation Damage to Ion Exchange Resin (W. C. Yee)

Sulfur determinations were made on new Dowex 50W X-12 (100-200 mesh) resin by both a combustion and a gravimetric method in order to check previously reported[25] results obtained by the standard Paar bomb method. An outline of the two methods of sulfur analysis is given below:

(1) Combustion method. This is a standard method used for determining carbon and sulfur content in steels. The resin sample is burned in an oxygen atmosphere in the presence of tin and copper oxide at temperatures as high as 1800°C. SO_2 gas given off is collected in a KI-starch solution which is then titrated with KIO_3 to give the amount of sulfur present as H_2SO_4.

(2) Gravimetric method.[26] The resin sample is treated with HNO_3, $HClO_4$ bromine-water and $BaCl_2$ in that order. The amount of sulfur present is determined by weighing the amount of $BaSO_4$ precipitated.

These results together with the Paar bomb results are given in Table 24. The calculated resin capacities agree with one another; however, they are all lower than the capacity of 5.1 ±0.3 meq/dry gram of resin specified by Dow Chemical Company.

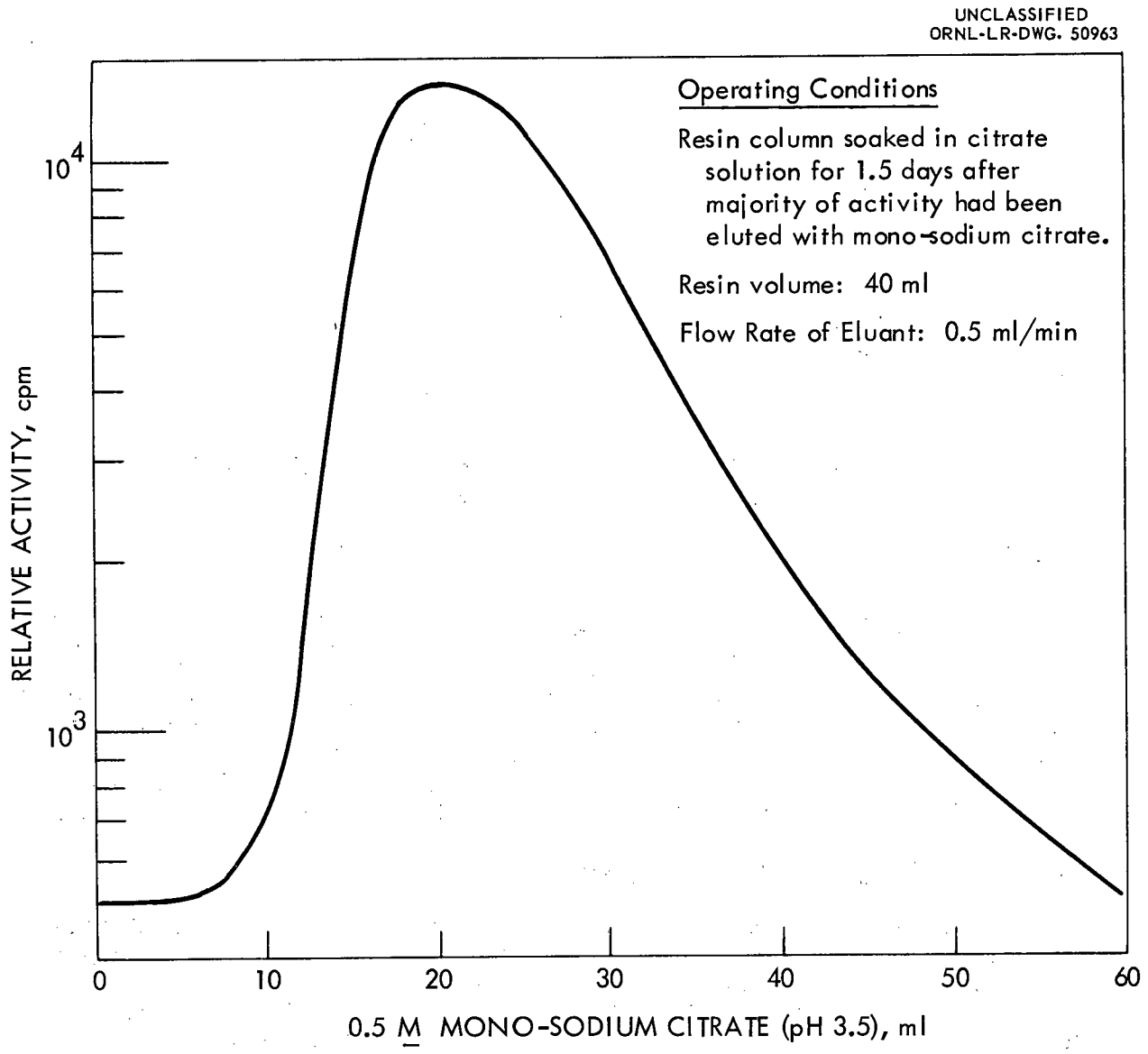

Fig. 30. Activity increase due to slow kinetics of citrate elution of rare earths from Dowex 50W X-12 (100-200 mesh) resin.

Table 24. Sulfur Analysis of Dowex 50W X-12 (100-200 mesh) Resin

Method	% Sulfur (dry basis)	Resin Capacity meq/dry gram of resin
Paar Bomb		
1	14.48	4.5
2	14.21	4.4
3	14.53	4.5
Combustion		
1	14.08	4.4
2	14.13	4.4
Gravimetric		
1	14.02	4.4
2	14.18	4.4
3	14.08	4.4
Dow Chemical Co. Specification	16 ±1	5.1 ±0.3

4.0 CHEMICAL APPLICATIONS OF NUCLEAR EXPLOSIONS (CANE)
(W. E. Clark, W. D. Bond)

4.1 Tritium Exchange

Tritium exchange from the water form to molecular hydrogen increased from about 0.07%/g $CaSO_4$ to about 2.7%/g of $CaSO_4$ when the temperature was increased from 380 to 700°C (Table 25). Due to large errors in counting statistics good agreement was not always obtained between the runs of low initial water specific activity and those of higher specific activity. The exchange rate reached a maximum after about 50 min operation and increased to this value according to the parabolic equation which indicates that the rate is controlled by bed diffusion (Fig. 31).

4.2 Reduction of $CaSO_4$ by Hydrogen

The rate of reduction of $CaSO_4$ by hydrogen under static conditions was virtually independent of hydrogen pressure in the 200-500 mm range (Fig. 32). It is not known whether the reaction is controlled by diffusion of gases to and from the reaction site, by adsorption of hydrogen, or by desorption of water vapor. The reduction rates at constant volume were 0.14 and 0.12 mm of hydrogen/min·m^2 for samples having surface areas of 2.9 and 0.82 m^2/g, respectively, which indicates that the reduction is directly proportional to the surface area. The progress of the reaction was followed by the pressure drop measured on a mercury manometer after trapping the water on a "drierite" trap.

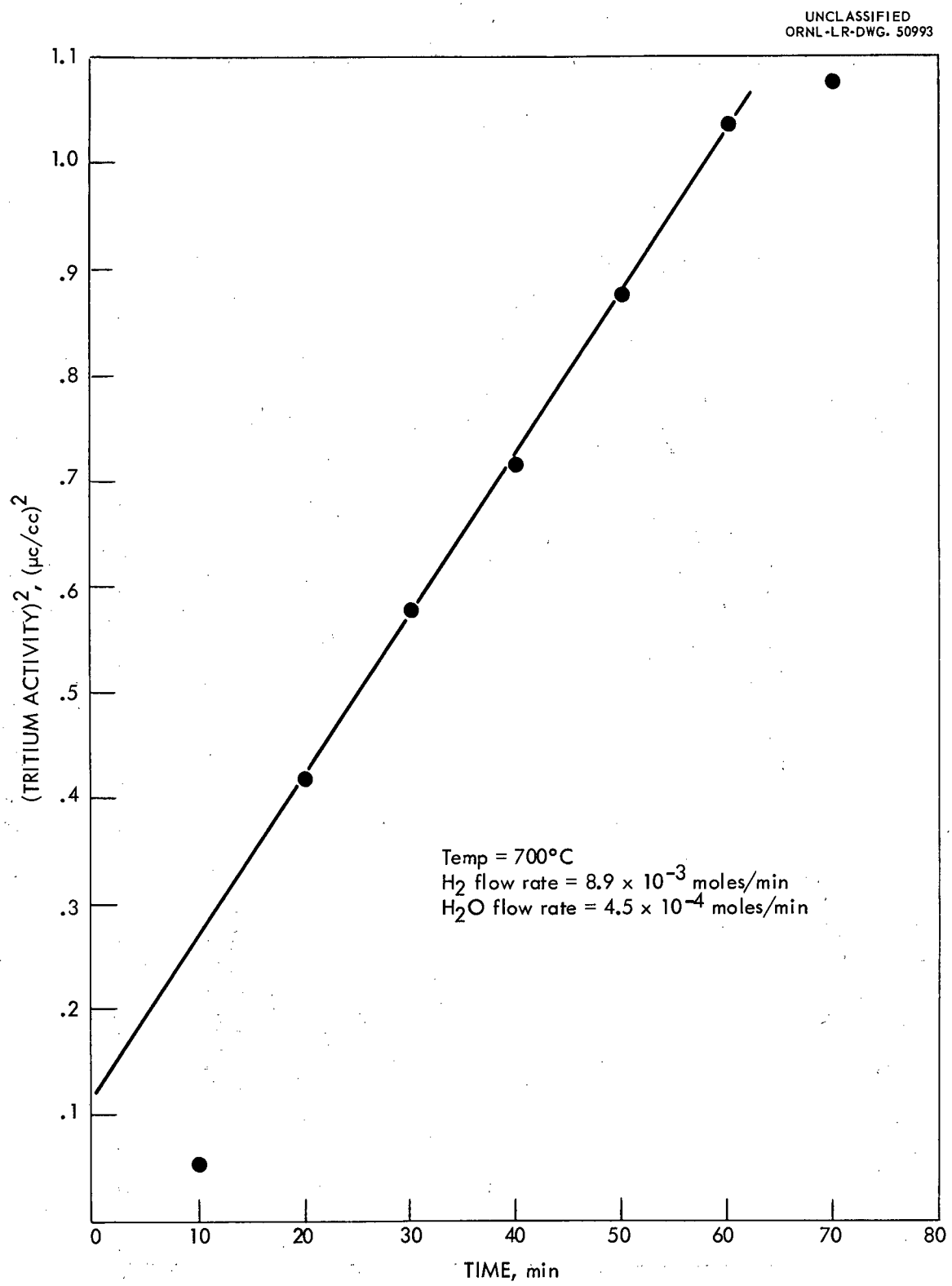

Fig. 31. Test of parabolic law for tritium exchange between water vapor and molecular hydrogen over calcium sulfate.

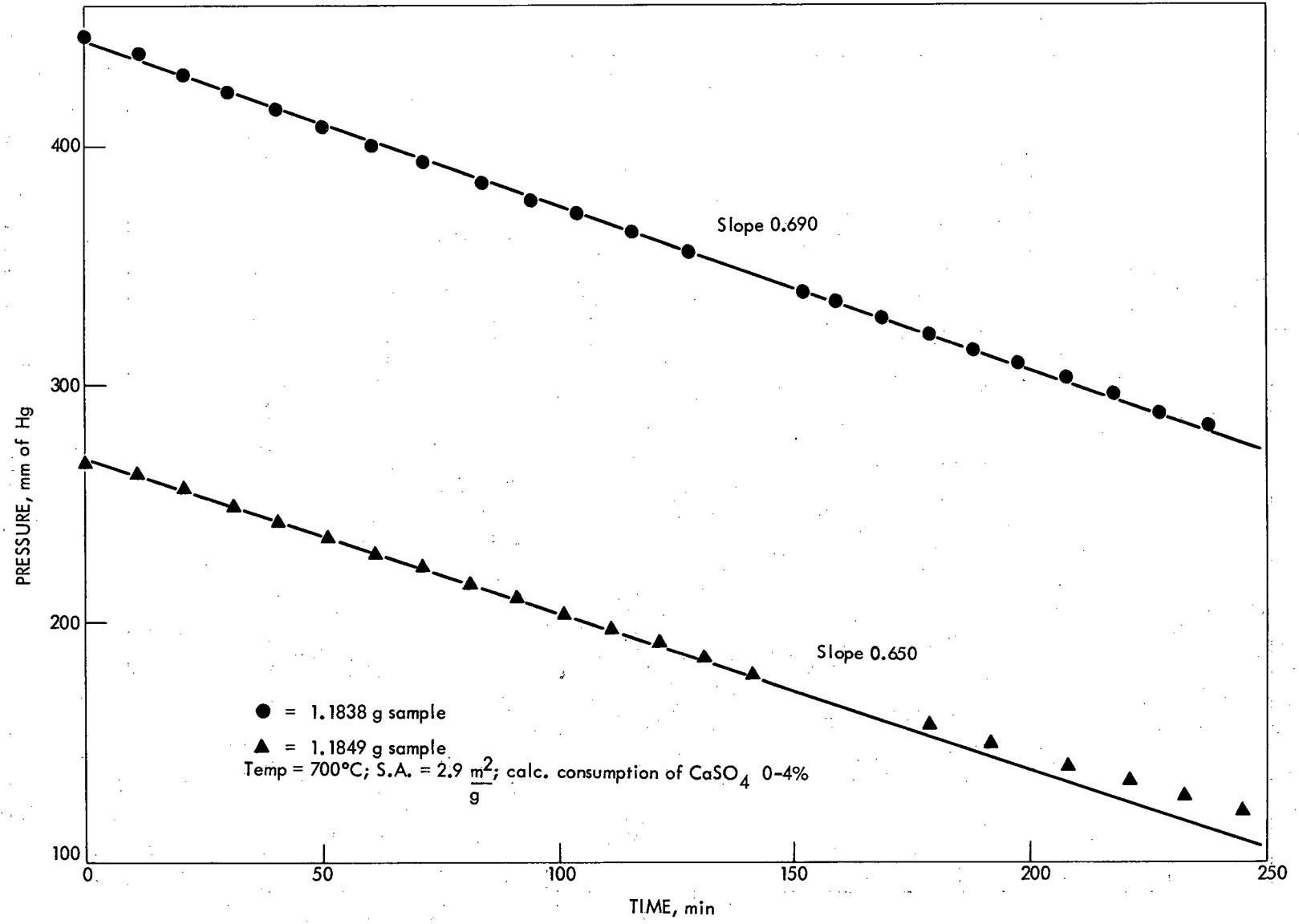

Fig. 32. Reduction of $CaSO_4$ by H_2 in static system.

Table 25. Exchange of HTO with H_2 Over Calcium Sulfate

H_2 Flow Rate = 8.9×10^{-3} moles/min
Tritiated Water Flow Rate = 4.5×10^{-4} moles/min
Reaction Time = 40 min
Surface Area of $CaSO_4$ = 0.82 m^2/g

Temp, °C	Init. Sp. Act. of Water μc/mole	Wt of $CaSO_4$ g	Tritium Exchange %	Tritium Exchange %/g of $CaSO_4$	Error due to Counting Statistics ± %
380	27.5	3.4248	0.03	0.0087	600
600	27.5	3.4248	3.96	1.156	5
600	27.5	12.45	11.92	0.942	20
700	27.5	3.4248	7.94	2.310	2
380	2650	2.7791	0.193	0.0694	0
600	2650	2.7791	5.32	1.914	0
700	2650	2.7791	8.10	2.915	0

4.3 Plasma Jet

$CaSO_4 \cdot 1/2\ H_2O$ powder passed through the plasma jet in a stream of argon gave a solid which reacted with water to give, within experimental error the theoretical alkalinity expected for CaO. Because of its hygroscopic nature, sodium chloride powders cannot be sprayed into the plasma jet in any controlled manner. After passing through the plasma jet, the salt was found to have an alkalinity of 3-6 x 10^{-4} milliequivalents per g.

A literature search revealed a new method[27] for measuring temperature of argon plasma in the 10,000-40,000°K range. It is based on the simultaneous measurement of the relative intensity of the 7635Å line of Ar and the 4806Å line of Ar^+.

4.4 Gnome Sampling

The thermal decomposition of ammonium bicarbonate is probably too slow for a "Filler" for the Gnome sampling pipe. Approximately 20 min were required to decompose 10 g of the material at temperatures in the 100-200°C range. The literature reports decomposition at 60°C but this is evidently too slow to be perceptible in a reasonable length of time. Ammonium bicarbonate was melted when sealed glass tubes containing the material were heated to 130°C.

5.0 REFERENCES

1. L. M. Ferris and A. H. Kibbey, "Sulfex-Thorex and Darex-Thorex Processes for the Dissolution of Consolidated Edison Power Reactor Fuel: Laboratory Development," ORNL-2934 (in press).

2. W. W. Schultz and E. M. Duke, HAPO, unpublished memorandum.

3. R. E. Blanco, L. M. Ferris, J. R. Flanary, F. G. Kitts, R. H. Rainey and J. T. Roberts, "Chemical Processing of Power and Research Reactor Fuels at ORNL," in "Proceedings of the AEC Symposium for Chemical Processing of Irradiated Fuels from Power, Test and Research Reactors," TID-7583, January 1960, p. 266.

4. Ibid., p. 261.

5. Ibid., pp. 238, 243.

6. W. Davis, Jr., "Radiation Power Densities in Future PRFR Pilot Plant 1AW Streams," ORNL-CF-59-3-78 (March 1959).

7. R. E. Blanco, L. M. Ferris, J. R. Flanary, F. G. Kitts, R. H. Rainey and J. T. Roberts, "Chemical Processing of Power and Research Reactor Fuels at ORNL," in "Proceedings of the AEC Symposium for Chemical Processing of Irradiated Fuels from Power, Test and Research Reactors," TID-7583, January 1960, p. 266, 268.

8. J. J. Perona, J. B. Adams, J. E. Savolainen and T. A. Gens, "Status of the Development of the Zircex Process," ORNL-2631 (March 1957).

9. T. A. Gens and R. L. Jolley, "New Developments in the Zircex Process," ORNL-2992, (in preparation).

10. J. E. Savolainen and R. E. Blanco, "Preparation of Power Reactor Fuels for Aqueous Processing," Chem. Eng. Prog. 53, 78-F (1957).

11. R. C. Reid, A. B. Reynolds, D. T. Morgan, G. W. Bond, Jr., J. E. Savolainen and M. L. Hyman, "Vapor-Liquid Equilibria of Dilute Nitric, Hydrochloric Acid, and Hydrochloric Acid-Nitric Acid-Water Solutions," Ind. Eng. Chem., 49: 1307-10 (1957).

12. M. J. Bradley and L. M. Ferris, "Recovery of Uranium and Thorium from Graphite Fuels. I. Laboratory Development of a Grind-Leach Process, ORNL-2761, March 17, 1960.

13. M. J. Bradley and L. M. Ferris, "Recovery of Uranium from Graphite Fuel Elements. III. Disintegration and Leaching with 90% Nitric Acid," ORNL-CF-60-3-65 (in press).

14. R. E. Blanco, "Monthly Progress Report for Chemical Development Section B, April 1960," ORNL-CF-60-5-106.

15. R. H. Rainey, A. B. Meservey and R. G. Mansfield, "Laboratory Development of the Thorex Process Progress Report, December 1, 1955 to January 1, 1958," ORNL-2591, p. 22.

16. R. E. Blanco, "Monthly Progress Report for Chemical Development Section B, May 1960," ORNL-CF-60-6-108.

17. R. E. Blanco, "Monthly Progress Report for Chemical Development Section B, March 1960," ORNL-CF-60-4-36.

18. R. E. Blanco, "Monthly Progress Report for Chemical Development Section B, April 1960," ORNL-CF-60-5-106.

19. R. E. Blanco, "Monthly Progress Report for Chemical Development Section B, May 1960," ORNL-CF-60-6-108.

20. L. H. Towle and R. S. Farrand, "Radiation Stability of Organic Liquids," Stanford Research Institute Semi-Annual Report No. 7, on Subcontract 1081, June 15, 1960.

21. R. E. Blanco, "Monthly Progress Report for Chemical Development Section B, April 1960," ORNL-CF-60-5-106.

22. H. W. Godbee and J. T. Roberts, "Survey on the Measurement of Thermal Conductivity of Solids Produced by Evaporation and Calcination of Synthetic Fuel Reprocessing Solutions," ORNL-2769 (Aug. 10, 1959) p. 15.

23. R. E. Blanco, "Monthly Progress Report for Chemical Development Section B, August 1959," ORNL-CF-59-9-16.

24. J. O. Blomeke and M. F. Todd, "Uranium-235 Fission-Product Production as a Function of Thermal Neutron Flux, Irradiation Time, and Decay Time," ORNL-2127 (August 1957).

25. R. E. Blanco, "Monthly Progress Report for Chemical Development Section B, February 1960,"ORNL-CF-60-3-84.

26. J. M. Chilton, "Quarterly Report for Period Ending September 10, 1951," ORNL-1129.

27. H. N. Olsen,"Thermal and Electrical Properties of the Argon Plasma," Linde Company Report (1959).

DISTRIBUTION

1. J. B. Adams
2-3. R. E. Blanco
4. J. O. Blomeke
5. J. C. Bresee
6. K. B. Brown
7. W. E. Clark
8. F. L. Culler
9. W. Davis
10. W. K. Eister
11. L. M. Ferris
12. D. E. Ferguson
13. J. R. Flanary
14. T. A. Gens
15. H. E. Goeller
16. A E. Goldman
17. J. M. Googin
18. A. T. Gresky
19. P. A. Haas
20. F. E. Harrington
21. R. F. Hibbs
22. J. M. Holmes
23. R. W. Horton
24. A. R. Irvine
25. W. H. Jordan
26. F. G. Kitts
27. Eugene Lamb
28. W. H. Lewis
29. R. B. Lindauer
30. A. P. Litman
31. J. P. Nichols
32. R. H. Rainey
33. J. T. Roberts
34. A. D. Ryon
35-37. E. M. Shank
38. M. J. Skinner
39. S. H. Smiley
40. E. G. Struxness
41. J. C. Suddath
42. J. A. Swartout
43. J. W. Ullmann
44. C. D. Watson
45. M. E. Whatley
46. C. E. Winters
47. R. G. Wymer
48. E. L. Anderson, AEC, Washington
49. R. F. Benenati, General Atomic
50. L. P. Bupp, Hanford
51. J. T. Christy, AEC, Hanford
52. V. R. Cooper, Hanford
53. F. R. Dowling, AEC, Washington
54. R. A. Ewing, BMI
55. M. K. Harmon, Hanford
56. B. R. Hayward, Atomics International
57. O. F. Hill, Hanford
58. K. K. Kennedy, ICPP
59. E. M. Kinderman, SRI
60. S. Lawroski, ANL
61. J. A. Lieberman, AEC, Washington
62. J. A. McBride, ICPP
63. B. Manowitz, BNL
64. J. W. Morris, du Pont, Savannah River
65. D. M. Paige, ICPP
66. H. Pearlman, Atomics International
67. C. A. Rohrman, Hanford
68. H. Shoen, RAI
69. C. M. Slansky, ICPP
70. K. G. Steyer, General Atomics
71. R. J. Teitel, Dow Chemical
72. V. R. Thayer, du Pont, Wilmington
73. J. Vanderryn, AEC
74. F. M. Warzel, ICPP
75. Document Reference Section
76-77. Central Research Library
78-82. Laboratory Records
83. ORNL-RC